Identification of the Role of A-To-I Editing in SINE RNA Stability

CODY R. TURNER
Bachelor of Science, University of Lethbridge, 2018

A thesis submitted
in partial fulfillment of the requirements for the degree of

MASTER OF SCIENCE

in

BIOCHEMISTRY

Department of Chemistry and Biochemistry
University of Lethbridge
LETHBRIDGE, ALBERTA, CANADA

Identification of the Role of A-To-I Editing in SINE RNA Stability

CODY R TURNER

Date of Defense: July 18, 2022

Dr. Athanasios Zovoilis Supervisor	Associate Professor	Ph.D.
Dr. Roy Golsteyn Thesis Examination Committee Member	Professor	Ph.D.
Dr. Trushar Patel Thesis Examination Committee Member	Associate Professor	Ph.D.
Dr. Michael Gerken Chair, Thesis Examination Committee	Professor	Ph.D.

Dedication

I would like to dedicate this thesis to my Grandmother.

Abstract

SINE RNAs are non-coding RNAs produced by Short Interspersed Nuclear Elements (SINEs), with SINEs of the B2 and Alu family being among the most frequent in mice and humans, respectively. Previous studies have shown that the processing of B2 SINE RNAs results in changes to the cellular stress response in mice through changes in the activation of stress response genes that are targeted by B2 RNAs. Thus, SINE RNA stability plays an important role in the regulation of gene expression. However, the factors that affect this processing are unclear. In this thesis, I investigated whether adenosine to inosine RNA modifications affects the stability of the B2 SINE RNA. To this end, optimization of solid phase RNA synthesis protocols for long RNAs that can incorporate the addition of inosines into the RNA sequence to generate *in vitro* synthesized B2 SINE RNA fragments with specific adenosine to inosine edits. In combination with ligation, complete *in vitro* synthesized B2 SINE RNAs were edited at specific positions and their processing rates could be compared to control synthesized B2 SINE RNA. Subsequently, expanded research into a cell culture model of neural cells and investigated how inhibition of A to I editing affects B2 RNA stability. The above study shows that A to I editing indeed affects the stability of the B2 SINE RNAs, and provides new insight into the mechanisms that affect overall SINE RNA stability.

Acknowledgements

I would like to thank Dr. Athanasios Zovoilis for all his assistance and guidance throughout this process, Luke Saville for the assistance and knowledge of laboratory equipment, Liam Mitchell for his computational assistance during this process, Travis Haight for his assistance in troubleshooting and general laboratory assistance, Chris Issac and Eric Merzetti for their assistance with thesis formatting and protocols, as well as all my lab members who helped to guide this project. Parts of this thesis have been or may be submitted for publication and constitute a collaborative work with members of the Zovoilis lab.

Table of Contents

List of Figures

List of Tables

List of Abbreviations

A to I	Adenosine to Inosine
APS	Ammonium persulfate
DMSO	Dimethyl Sulfoxide
dsRNA	Double-Stranded RNA
EDTA	Ethylenediaminetetraacetic acid
LINE RNA	Long interspersed nuclear elements
lncRNA	Long non-coding RNA
mRNA	Messenger RNA
miRNA	Micro-RNA
m6A	N^6-methyladenosine
ncRNA	Non-coding RNA
PAGE	Polyacrylamide Gel Electrophoresis
PCR	Polymerase Chain Reaction
qPCR	Quantitative Polymerase Chain Reaction
rRNA	Ribosomal RNA
RNAi	RNA-mediated interference
siRNA	Small interfering RNA
SINE RNA	Small-interspersed nuclear elements RNA
snoRNA	Small nucleolar RNA
tRNA	Transfer RNA
TBE	Tris base, boric acid, EDTA
TEMED	N, N, N', N'-tetramethylethylenediamine

Chapter 1

Introduction

1.1 Non-coding RNAs

1.1.1 Definition

For many years, various classes of non-protein coding RNAs (non-coding RNAs, ncRNAs) were regarded as non-functional by-products of the non-coding genome otherwise referred to as the products of "Junk DNA". The focus has been instead on the protein-coding regions of the genome, which were being intensely studied for their ability to code for a variety of proteins, despite only representing <2% of the total genome (Wilusz et al. 2009). In contrast, ncRNAs represent a diverse class of RNAs that slowly are being revealed to be responsible for many of the cellular functions found within all domains of life (Cech and Steitz 2014). Research into various classes of ncRNAs has shown considerable promise for their use as a therapeutic agent and aa biomarkers for diagnosis (Santer et al. 2019).

ncRNAs can be separated into two main types. The first type and often most extensively studied is that of the structural ncRNAs including ribosomal RNA (rRNA), transfer RNA (tRNA), and small nucleolar RNA (snoRNA). All of these have well-established roles in cellular development, from translation and splicing to RNA sequence recognition (Phizicky and Hopper 2010) (Yan et al. 2019). While the structural ncRNAs function has been well established, due to their clear functional roles, they are not the only major category of ncRNAs. The second type of ncRNAs includes RNAs such as small interfering RNA (siRNA), small-interspersed nuclear elements RNAs (SINE RNA), long non-coding RNAs (lncRNA), along with a variety of other diverse

ncRNAs (Pertea 2012). This second major group of ncRNAs have been classified as regulatory RNAs since they perform regulatory cell functions through structural and base-pairing interactions, to control a variety of cellular functions (Mattick and Makunin 2006).

1.1.2 Regulatory ncRNAs

Regulatory ncRNAs include, among others, small regulatory ncRNAs which are divided into two main classes: 1) microRNA/small interfering RNA (miRNA/siRNAs) - responsible for degradation or translational repression of mRNAs (Correia de Sousa et al. 2019) (Reynolds et al. 2004), and 2) small nucleolar RNAs (snoRNAs) – responsible for RNA editing most notably in that of ribosomal RNA (rRNA) - and small nuclear RNAs (snRNAs) (Xing and Chen 2018). Another class of regulatory ncRNAs is produced from repetitive genomic elements, which were once considered transcriptional noise and a by-product of evolution. Repetitive genomic elements, such as Short Interspersed Nuclear Elements (SINEs) do not encode for proteins despite encompassing around one-third of the entire human genome and being found in almost all eukaryotes (Weiner 2002). Transcripts from these elements were regarded initially as not playing a direct role in cellular function as they did not code for messenger RNA (mRNA) (Mattick and Makunin 2006).

1.1.3 LINEs and SINEs RNAs

Long Interspersed Nuclear Elements (LINEs) and Short Interspersed Nuclear Elements (SINEs) have had a major effect throughout the evolution of the mammalian genome due to their innate retrotransposon activity (Bodea et al. 2018). LINEs are capable of encoding for their retrotransposon and thus capable of retro-transposition, while SINEs remain non-autonomous relying on LINE retrotransposons (Richardson et al. 2015). Despite being regarded as part of "Junk DNA", the repetitive genomic elements under the classification of LINEs and SINEs have recently been assigned roles across various disease and immune response activities. For example, in the case of LINEs, it is estimated that among spontaneous disease-producing insertions in humans approximately 1 out of 1000 could be attributed to the long interspersed element-1 (LINE-1) (Beck et al. 2011).

While SINE elements remain less autonomous and have a reduced capacity for retrotransposon activity, they make up a larger proportion of the genome and are responsible for a wide arrangement of cellular activities. SINEs are actively transcribed through RNA polymerase III, allowing them to generate short ncRNAs called SINE RNAs. The SINE encoded ncRNAs are typically smaller than 500 bp despite being found in large copy numbers throughout the human genome (Tucker and Glaunsinger 2017). A major SINE element family is derived from the 7SL RNA, which evolved independently in some eukaryotes, giving rise to a branch in the mammalian line between rodents and primates. In primates including humans, this gave rise to the ALU family of SINE elements, while in rodents they gave rise to the B1 SINE elements. However, rodents' genomes also include transfer RNA (tRNA) derived SINE elements called B2 elements (Karijolich et al. 2017).

1.2 RNA Modifications

1.2.1 The emergence of RNA modifications and the epi-transcriptome

The diversity in RNAs is vastly expanded through chemical modifications that have a significant impact on the structure and function of a large variety of RNAs. Initially, RNA modifications were described to be caused by structural changes observed in many ncRNAs such as tRNAs and rRNAs (Jonkhout et al. 2017). This notion was further adapted when reversible modifications were discovered adding additional complexity to the effects of RNA modification and constituting what is known as the epitranscriptome (Jia et al. 2013). This complexity has led to renewed interest in the impact that RNA modifications have across all forms of RNA, and their potential implications in what was previously categorized as an epigenetic disease (Zhang et al. 2020). Furthermore, the creation of RNA modification databases (Boccaletto et al. 2018) has provided an essential tool in the study of disease as many modifications have been overlooked due to the difficulty of eluding their location and their role in the genome. Thus, a greater understanding of RNA modifications may allude to the hidden roles they play in the evolution of species and the occurrence of some spontaneous diseases (Barbieri and Kouzarides 2020).

1.2.2 The role of RNA modifications in ncRNAs

RNA modifications have been found throughout a diverse range of RNAs with most forms of RNA experiencing some form of modification. Initially, tRNAs were found to harbour many modifications during their maturation process as far back as the first sequencing of biological RNA in 1965 (Roundtree et al. 2017). Shortly after, the wide variety of sequencing and RNA assays led to the discovery of modifications being found throughout most RNA species. In particular,

double-stranded RNA (dsRNA) was found to be highly edited across most eukaryotes, with the editing being responsible for post-transcriptional gene regulation. This regulation allows cells to direct mRNA structure, export nucleolar RNA, facilitate transcription and translation, as well as, a large array of other functions (Zhao B. S. et al. 2017). The importance of RNA modifications in gene regulations is exemplified by RNA-mediated interference (RNAi) which is capable of quickly silencing genes alongside various enzymes by targeting RNA transcripts for degradation (Gavrilov and Saltzman 2012) (Agrawal et al. 2003). This role in the control of gene expression is exemplified with modifications in miRNAs which undergo RNA modifications during their maturation process, while misedited transcripts may lead to a variety of impairments in brain function and development (Correia de Sousa et al. 2019). Furthermore, regulation by RNA editing has many implications when reviewing all ranges of eukaryotes and specifically during development where retrotransposable elements being highly edited are associated with distinct editing profiles which may cause dysregulation and disease throughout the lifecycle of an organism (Zhou et al. 2020).

1.2.3 Diversity of RNA modifications

The number of known RNA modifications remains vast with at least 100 different unique modifications described (Zhao B. S. et al. 2017). Like in DNA modifications, methylation is found in many different RNA species with the most prevalent being the N^6-methyladenosine modification(m6A) found in most species of mRNA. These m6A modifications are responsible for a variety of epigenetic changes required for mRNA maturation, cell differentiation, and disease progression (Zhao L. Y. et al. 2020) (Sun et al. 2019). Other adenosine modifications such as m1A, where the methyl group is attached at the N^1 position, are prevalent in rRNA and tRNA despite

still being found within mRNA (Dominissini et al. 2016). Conversely, methylation is not present only in adenosine bases, but also across most bases, such as C, with m5C being common across tRNA, mRNA, and rRNA. The m5C methylation is important for a variety of functions within eukaryotic RNA, important for cell growth and differentiation, while also being responsible for the wobble base pair in some tRNA (Squires et al. 2012).

Structural RNAs such as tRNAs require a vast host of modifications for their maturation to occur. One of these essential modifications is pseudouridine which is a modified uridine base that is modified during the maturation of RNA including rRNA (Perks et al. 2018) and tRNA (Soll 1971) among others. Due to pseudouridine's effect on the sugar-phosphate backbone structure, it imparts structural importance to the maturation of RNA molecules (Charette and Gray 2000). Furthermore, tRNA undergoes a long maturation process requiring many modifications where a mature tRNA may contain up to 25% of its total nucleotides being modified. The large modification numbers in tRNAs led them to be intensely researched, however many other ncRNAs were left out of the important picture of RNA modification due to their low number along with being considered "Junk DNA/RNA" (Helm and Motorin 2017).

Interestingly, inosine modifications were found relatively early across various classes of RNA, particularly in many ncRNAs. The Adenosine to Inosine modification (A to I) is the result of the deamination of adenosine resulting in a new base that is recognized by both sequencing and cellular machinery as guanosine (G) (Xu and Ohman 2018). The changes in recognition play important roles in changing the function of coding and non-coding RNAs, by affecting splice sites, codons, secondary structure, and self-recognition impacting interferon response (Brachova et al. 2019). Furthermore, with the advent of full genome sequencing and bioinformatics, it was

determined that greater than 90% of all inosine editing in humans was found to fall within the primate-specific SINE element Alu.

1.3 Role of SINE RNAs in cell function

1.3.1 Origins

SINE elements are transposable elements found in high copy numbers originating from tRNA, 7SL RNA, and 5S rRNA, and are found throughout higher eukaryotes (Ustyantsev et al. 2020b). These transposable elements make up around 40% of long-noncoding RNAs (lncRNA) being found as both isolated transcripts as well as functional domains on lncRNA (Fasolo et al. 2019). Due to their vast copy numbers and functions, it has been hypothesized that SINE elements may play a great role in the evolution of species by having a direct impact on gene expression, insertions, and recombination leading to changes within the genome (Batzer and Deininger 2002).

The vast expansion of SINE elements can be easily identified within mammals. In humans, Alu repeats represent the main category of SINE elements. The Alu family of SINE RNA is approximately 300bp in length and with copy numbers reaching over one million, Alu repeats have proliferated due to their ability to duplicate through retrotransposon activity though not independently. While the Alu elements are primate-specific they are classified into different Alu subfamilies because of their diverging sequence (Salem et al. 2003). This diversity among Alu throughout millions of years has led to genome changes within primates giving distinct Alu RNA repeats allowing for the proliferation of new species through their diverging genetic structure (Carroll et al. 2001).

Like primates, the family of rodents have their SINE elements proliferating during the branch from the mammalian line with the SINE family of elements B1 and B2 being the main representatives. The rodent SINE elements share many of the ALU characteristics, such as their large copy number and major proliferation during times of heavy genomic changes. Furthermore, rodent SINE B1 elements share a similar predecessor to the Alu family of SINEs, both originating from the 7SL rRNA. However, in the case of rodents the many B1 transcripts are now considered inactive (Yang L. et al. 2019). In contrast, the members of the B2 family of SINEs in rodents owe their origins to tRNAs unlike that of the primate Alus, though they remain highly active (Daniels and Deininger 1985).

1.2.3 Transcription of SINE RNAs

SINE RNAs including ALU, B1, and B2, among others, have been shown to possess a significant role in cell function and regulation of gene expression (Elbarbary et al. 2016). There are two main methods for SINE RNA transcription. Firstly, many SINE RNA are transcribed into active transcripts by the process of intron splicing where intron bound SINEs are spliced out of mRNA (Yu and Zhang 2005). Secondly, many SINE transcripts are produced through a Polymerase III related transcription like that of tRNA including polyadenylation (Borodulina and Kramerov 2008, Ustyantsev et al. 2020a).

1.3.2 Functional roles of SINE RNAs

Transcription of SINE RNAs is an important factor in the control of cell function exemplified by their roles in stress and anti-viral response. In mouse cells, transcribed B2 RNA is found bound to heat shock-responsive genes in both intergenic and intronic regions. In these

regions, B2 is found in the pre-initiation complex of RNA polymerase II acting as an inhibitor of immediate early gene transcription. Thus, B2 cleavage as catalyzed by EZH2 results in the activation of stress-related genes allowing for an immediate-early response to external stress (Zovoilis et al. 2016). Furthermore, SINE RNAs including B2 and ALU RNAs are self cleaved representing a large proportion of ribozyme activity within the cell. This self-cleavage mechanism is accelerated 100-fold during stress by EZH2 allowing for rapid response and cleavage of the B2 RNA. This cleavage of the B2 SINE alleviates the gene repression of heat-shock genes and within 15 minutes of the stress occurring allows for rapid cellular response (Hernandez et al. 2020).

SINE RNAs remain a hotspot for modifications, contributing to their vast array of functions and diversity. One of the many modifications to SINE RNA is A to I editing with as many as 90% of known A to I editing sites being found directly within mammalian SINE elements. One of the major roles of A to I editing in SINE RNAs is intron splicing, as the modification is capable of creating 5’ GU or add or remove 3’ AG splicing sites that result in a change of the intron splicing sites. (Mallela and Nishikura 2012). Therefore, some intronic Alu transcripts are retained within functioning mRNAs allowing for further regulation, as inosine edited Alus provide a domain within the transcript for the protein P54 to bind and promote nuclear retention. This retention allows for control over which transcripts can actively be translated, while the retained pre-mRNA transcripts may be held within the nucleus as pre-transcribed stress response and cell cycle genes (Chen and Carmichael 2008). Furthermore, modification of SINE RNAs may have a greater direct impact on the life cycle of this RNA, as highly edited double-stranded RNA (dsRNA) inhibits interferon signalling allowing for free RNA to inhabit cytoplasmic tissues without rapid degradation. Inversely, endonuclease V has been identified to be responsible for the degradation

of highly edited Alu dsRNA, resulting in both the regulation and control of interferon signalling, thus, implicating an important regulatory role of A to I editing patterns of SINE RNAs (Nishikura 2016).

1.4 Adenosine to Inosine modifications and SINE RNAs

1.4.1 Adenosine to Inosine chemical modifications

Adenosine to Inosine editing was first discovered due to its ability to unwind RNA duplexes as a result of the change causing hairpin mismatching, while the editing activity has been known to be specific to dsRNA (Walkley and Li 2017). The transition from adenosine to inosine is the result of deamination at the N6 position catalyzed by the adenosine deaminases acting on RNA (ADAR) protein family which are responsible for all A to I editing (Figure 1.1) across most animals (Li et al. 2019). The deamination results in the base being recognized by sequencing and cellular mechanisms (including translation) as guanosine effectively acting as a substitution with the ability to bind cytosine (Teichert 2018). Thus, this modification can create and remove the secondary structure of RNAs by disrupting or creating new dsRNA sections and hairpins.

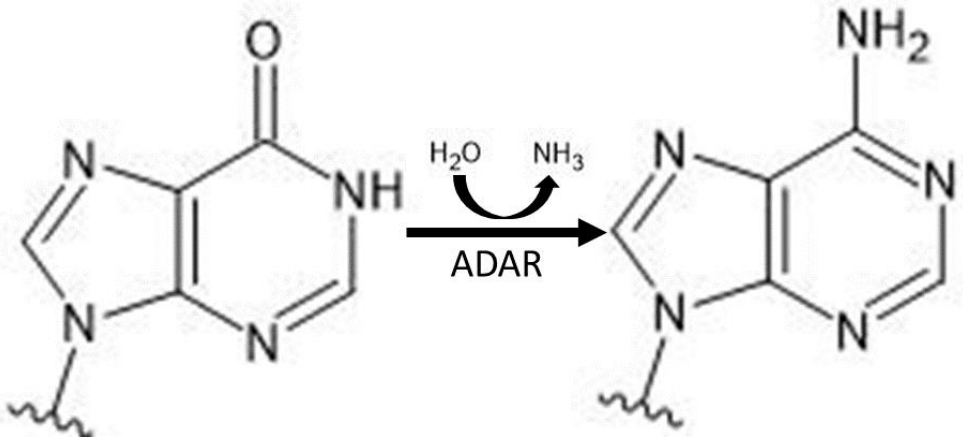

Figure 1.1: Adenosine to Inosine conversion catalyzed by the ADAR family of enzymes. Figure created by ACD/ChemSketch FreeWare (Advanced Chemistry Development 2021).

1.4.2 ADAR enzyme family

The ADAR family of enzymes is comprised of 3 enzymes: ADAR1, ADAR2, and ADAR3. The first form of ADAR1 is comprised of two main isoforms p110 and p150, having different locations within the cell with the p110 being found within the nucleus, while the p150 transcript is found to be transported between the nucleus and cytoplasm (Sun et al. 2021). Due to its location, the p110 is mainly responsible for the ADAR1 editing of nuclear transcripts including intronic SINE RNAs required for nuclear retention of transcripts (Hong et al. 2015). Conversely, in the cytoplasm, the p150 transcript is solely responsible for editing along with their ability to bind to Dicer and promote cleavage resulting in an anti-viral response while also marking edited RNA as self transcribed RNA (Licht et al. 2019). This promotion of RNA interference (RNAi) is antagonistic to A to I editing of RNAs, resulting in transcripts that have been edited being able to avoid dicer machinery due to their dsRNA structure (Ota et al. 2013). Similarly, ADAR2 is also catalytically active within many species but is responsible for a smaller number of total edits than that of ADAR1. However, it does still play an important role in editing as the dysfunction of ADAR2 may

result in a variety of misedited transcripts resulting in a variety of diseases (Moore et al. 2019). In contrast, ADAR3 is catalytically inactive but is still expressed within the nucleus of brain tissue in mammals. Furthermore, unlike ADAR1 and ADAR2 deficiency leading to death in mice, ADAR3 deficient mice are viable, however, they begin to exhibit behavioural and cognitive dysfunction. This observation led to further understanding of the role ADAR3 may play in learning and gene regulation (Mladenova et al. 2018).

1.4.3 Location of edits

A to I modifications are found throughout many different regions of the transcriptome including coding and non-coding RNA. As the ADAR family of enzymes only targets adenosine bases on dsRNA the modifications can be found in most double-stranded adenosines, however, the editing rate can be impacted by upstream and downstream structure (Eggington et al. 2011). ADAR1 plays important role in anti-viral defence with ADAR transcripts being increased while treated with interferon, facilitating modification of viral RNA transcripts, while also playing an important role in the maturation of pre-mRNA intron splicing (Samuel 2001). Furthermore, increased A to I conversion along long dsRNAs due to ADAR activity shows a reduction in Dicer conversions to siRNA, while this may also have a direct impact on siRNA targeting as a single A to I conversion may prevent siRNA activity (Nishikura 2010). However, in the case of mRNAs, most of the A to I conversions are found within the non-coding regions of introns and UTRs. Within these non-coding regions, there are many copies of SINE and LINE elements, with some studies showing that over 90% of all A to I edits in humans may be found within Alu sequences. Thus, edited SINE Alu sequences, when found in introns are shown to have an important effect on pre-mRNA splicing, while also affecting nuclear retention when found in UTRs (Yang Y. et al. 2013).

1.5. Rationale and aims of the current Thesis

1.5.1 Rationale

As mentioned above, several previous studies have revealed the important role of B2 SINE RNAs in the control of stress-response genes in mouse cells. In particular, B2 SINE RNAs were found to bind RNA Polymerase II at stress response genes resulting in transcriptional suppression. During heat-shock stress the B2 RNA is processed by interactions with the EZH2 protein and cannot bind RNA Polymerase II anymore, allowing for the transcription of genes associated with the stress response (Zovoilis et al. 2016). Furthermore, the human SINE Alu RNAs were also linked to processing during studies involving thermal stress increasing stress-response genes. As well, the binding interaction of EZH2 with the mouse SINE B2 and the Alu were both found to have their self-cleaving activity accelerated (Hernandez et al. 2020).

The identified interactions between SINE RNAs and the transcription of stress-response genes raised the prospect of a potential role of SINE RNAs in human disease. Recent studies from the Zovoilis Lab in mouse models of Alzheimer's Disease using APP+ mice showed an increase in the processing of B2 SINE RNAs during the active neural degeneration phase, induced by amyloid beta toxicity, which leads to an increase in overall B2 processing (Cheng et al. 2020). In addition, similar pathways were found in human SINE ALU RNAs, for which an increased SINE RNA processing rate was found in Alzheimer's disease patients' brains (Cheng et al. 2021). This increase in processing of SINE RNAs implicated changes in SINE RNA stability and processing may be important for regulating gene expression in AD patients, as increased processing of SINE RNA

results in the increased gene expression of stress response genes found in Alzheimer's Disease (Cheng et al. 2021).

Through the above-mentioned studies, the processing of SINE RNAs has been connected with the response of neural cells to amyloid beta toxicity in Alzheimer's disease mouse models (APP+ mice) and patients (Cheng et al. 2020) (Cheng et al. 2021). Furthermore, glutamate cycles are dysregulated within Alzheimer's disease giving an application to study *in vivo* cell cultures during cellular stress comparable to that of our model (Andersen et al. 2022). To this end, elucidating the factors that regulate SINE RNA processing and stability is important for understanding this novel mode of gene expression regulation and the disease that its deregulation may cause.

As outlined in sections 1.2 and 1.4, A to I editing could be a factor that affects SINE RNA stability. In particular, A to I editing and the resulting changes in base pairing have been described to affect RNA stability and function. For example, in the case of viral RNAs, A to I editing has been shown to induce stability or alter the structure irreversibly (Liu et al. 2019) (Netzband and Pager 2020). I-C bonds show increased thermal stability even compared to that of G-C bonds of dsRNA (Wright et al. 2018). Thus, due to the increased stability of I-C bonds found within dsRNA, they may play a role in the stability of rapidly self-degrading ribozymes such as SINE RNAs.

As mentioned above, the processing of SINA RNAs is critical for their function in neural cells during amyloid beta toxicity. In addition, preliminary data from our lab have revealed that inosine editing events are altered in Alzheimer's mouse models (APP+ mice) (Figure 1.2) at 3-month-old mice compared to the respective wild type mice (WT) of the same age (Mitchell et al,

submitted). Furthermore, 6-month APP+ mice also depict increased rates of editing at position 49 of the B2 SINE RNA, however, at a lower rate than in 3-month mice. In contrast, after 12 months the editing of the B2 SINE RNA no longer shows a significant difference in position 49 between APP+ mice and WT mice (Mitchell, et al, submitted). SINE RNA processing levels are increased in 6-month-old APP mice but not in 3-month-old mice implicating that an increase in A-to-I editing in 3-month-old mice may play a role in reducing the processing of B2 SINE RNAs in that age compared to 6-month-old mice (Cheng et al. 2020). Thus, RNA Adenosine to Inosine editing may be implicated in the overall stability changes found in B2 RNAs. Furthermore, the increase of A to I activity within SINE transcripts of intronic B2 and Alu RNA may involve the ADAR family of enzymes as a regulatory element of the ribozyme self-cleaving activity of SINE RNAs.

However, the above association of A to I editing with B2 RNA processing has been described only *in vivo* and we currently lack any mechanistic confirmation of this association in the controlled setting of *in vitro* experiments that would expand our knowledge of the impact that A to I editing has upon SINE RNAs. To this end, cell culture assays would allow us to gain a deeper understanding of the importance of the Inosine modification on B2 RNA stability and look at the regulatory effects that ADAR enzymes may have on overall B2 stability. Thus, the introduction of *in vitro* cell culture analysis in the HT22 hippocampal cell line allows us to study neural cells to mimic Alzheimer's disease tissues. Furthermore, due to its reactions with tau oligomers the antitumor suppression gene p53 is an important gene in AD models as both an important stress response candidate to ensure adequate stress to cellular components as well as, to uncover any affect that the reduction in A to I editing may have on overall p53 expression (Gadhave et al. 2022). In addition, *in vitro* biochemical assays would allow us to study the impact

of Inosine modifications directly on the B2 RNA, and to this end, in vitro modified B2 RNA would need to be created using solid-phase RNA synthesis. To address these challenges, the current Thesis was designed around two main aims that are outlined in the next section.

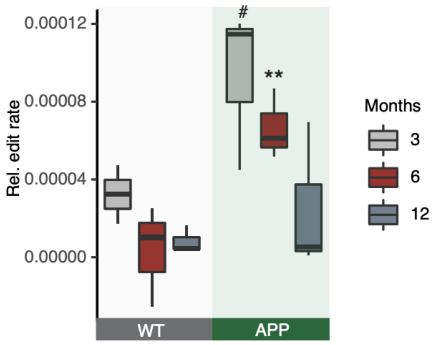

Figure 1.2: Relative editing rate in both Wild Type and APP mice at B2 Position 49. Two asterisks represent statistical significance for the comparison between the six-month mice (p=0.03, unpaired non-directional t-test WT-n=3 APP-n=3). Pound sign (#) represents statistical significance between 3-month mice (p=0.05, unpaired directional t-test, WT-n=2 APP-n=3) (Mitchell et al, submitted)

1.5.2 Aims

Cellular stress induction of SINE RNA cleavage is rapid and essential. A to I editing may provide essential stability to SINE RNAs and prevent rapid self-ribozyme activity. Thus, we hypothesize a connection between conserved A to I editing sites of B2 SINE RNA and the stability of B2 RNA structure and sequence. Based on this hypothesis, the aims of this thesis are to:

1. Investigate whether changes in A to I editing have a direct impact on the processing rate of *in-vitro* synthesized B2 SINE RNAs.

2. Investigate the effect that changes in A to I editing through inhibition of ADAR enzymes have on SINE processing rates *in vivo* in a cell culture model.

Chapter 2

Methods

2.1 Solid phase RNA synthesis

2.1.1 In Vitro Design

To test the impact of A to I edits in B2 RNA processing, firstly we needed to synthesize B2 RNAs in vitro that include Inosines at certain positions. Figure 2.1 depicts our experimental strategy regarding this.

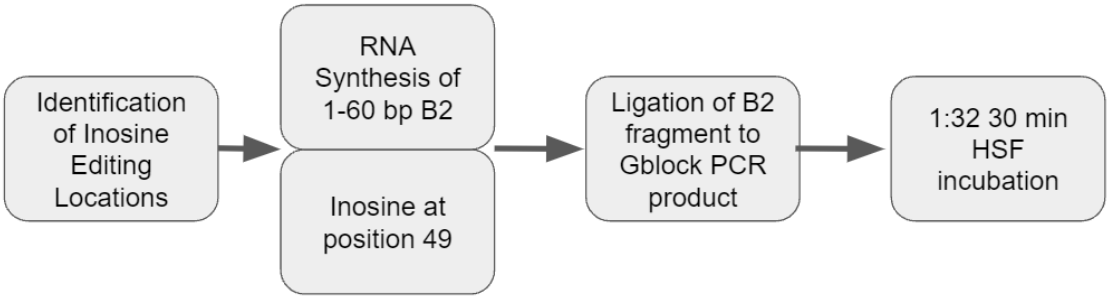

Figure 2.1: Experimental Design of In Vitro synthesis of Inosine containing B2 and 1:32 HSF-1 incubation assay.

2.1.2 RNA synthesis

Inosine modified SINE RNAs were generated using solid-phase RNA synthesis on a K&A GHR H-8 synthesizer. RNA synthesis was performed using TBDMS protected ACGT Amides (Glen Research), Universal Support III Columns (Glen Research), TCA deblock (Trichloroacetic acid/Dichloromethane 3/100 (v/v)) (Sigma), Acetonitrile, anhydrous 99.8% (Sigma), ETT activator (0.25 M) (Sigma), Oxidizer (Tetrahyrofurane/Water/Pyridine/Iodine 77/2/21/2.54 (v/v/v/w) (0.1 M)) (Sigma), Cap A (Acetic Anhydride/Tetrahydrofurane 9.1%/90.9%) (Sigma), Cap B (Acetonitrile

/ N-Methylimidazole(Sigma). Before synthesis, the RNA synthesis trityl monitor is cleaned by automatic device operations. Amides are resuspended in Acetonitrile to 0.067 M for expedite synthesizers. Once resuspended amides are added to the synthesizer and primed three times to ensure air is flushed from the system. Synthesis occurs one base at a time in a 3' to 5' direction using the K&A H-8 synthesizer. Synthesis of RNA amides follows a 4-step synthesis process, 1) Deblocking – 44seconds, 2) Coupling - 800 seconds, 3) Coupling – 30 seconds 4) Oxidation – 318 seconds. For RNA Synthesis a coupling time of 800 seconds is used while DNA synthesis uses a 30 second coupling time. Following synthesis RNA remains bound to Universal Support III Columns, requiring column extraction and deprotection.

2.1.3 RNA synthesis, column extraction and deprotection

Post-synthesis, the RNA-bound columns were dried for 24 hours at 4 ^{o}C. Subsequently, the column substrate was extracted by penetration of the column cap and transferred to screw-cap tubes. To each tube, 200 µL of 2 M ammonia in methanol (Sigma) was added and incubated at room temperature for 1 hour. Deprotection of trityl-attached base of the RNA bases was done by addition of 1.5 mL solution of AMA (Sigma) incubated for 10 minutes at 65 ^{o}C. Following incubation, the solution was cooled to room temperature. The cooled samples were decanted and allowed to dry at room temperature.

Following the drying process, a second round of deprotection to facilitate the removal of 2' protecting group TBDMS was applied. The dried solution was resuspended in 100 µL of anhydrous DMSO (Dimethyl Sulfoxide) (Fisher) and heated at 65 ^{o}C for 5 minutes to facilitate resuspension. Once the RNA was fully resuspended the solution was added to 125 µL TEA

(Triethylamine) (Sigma) and incubated at 65 ^{o}C for 2.5 hours and allowed to cool at -20 ^{o}C for 1 hour.

Following deprotection desalting of deprotected RNA was required. The deprotected RNA was vortexed with 25 µL 3 M Sodium Acetate (Sigma), followed by 1 mL 1-butanol (Sigma), and vortexed a second time. The mixed RNA solution was cooled at -80 ^{o}C for 30 min before the RNA was pelleted by centrifugation for 10 minutes at 12500 rpm. The pellet was then decanted off the butanol with a pipette before being cleaned with two washes of 0.75 mL of 80% ethanol, which were both decanted off using a pipette. The pellet was allowed to air dry for 15 minutes before being resuspended in 400 µL of Ultra Pure Distilled Water (Invitrogen). After being fully resuspended, it was stored at -80 ^{o}C before undergoing further purification.

2.1.4 Purification of Synthesized B2 RNA

Following extraction and deprotection, the synthesized RNA samples require additional size selection using PAGE gel extractions. The gel extractions required the staining of 10% Urea PAGE gel and excision of the band of interest (60 bp) using gel imaging. Each band of interest was placed into a microcentrifuge tube along with 400 µL of gel extraction buffer containing Tris-HCL (20 mM) (Invitrogen), Sodium Acetate (0.3 M) (Sigma), and EDTA (1 mM) (Invitrogen). Each tube was frozen at -80 ^{o}C for 15 minutes before being placed on a shaker table and allowed to diffuse at room temperature for 20 hours. Following the 20 hours at room temperature, each tube was pelleted in by centrifugation for 10 minutes at 13000 rpm. The supernatant from each sample was removed and Sodium Acetate (1M) (Sigma) was added to 0.3 M final concentration, along with 2.5 times the volume of 100% ice-cold ethanol. The RNA solution was chilled at -80 ^{o}C for

20 hours, before being pelleted by centrifugation for 5 minutes at 13000 rpm, before being decanted with a pipette. Each RNA pellet was washed twice with 1 mL of 80% ethanol and allowed to air dry for 15 minutes. After the pellet was dried it was resuspended in 10 µL of Ultra Pure Distilled Water (Invitrogen), to be used in ligations to allow for full-length modified B2 RNA.

2.1.5 In Vitro Transcription

In vitro transcription (IVT) was performed using specific gBlock DNA reference sequences (IDT) (Table A.2). The following IVT was performed using the Hi-Scribe kit (NEB) with a working sample containing 1.5 µL of each RNA triphosphate (ATP, CTP, UTP, and GTP (7.5 mM)), 1.5 µL of Hi-Scribe buffer, 1 µg of DNA template, with the addition of H_2O up to 20 µL. The total solution was incubated at 37 ^oC for 4 hours before being gel purified.

B2 RNA of non-edited regions of the RNA was obtained via in vitro transcription using T7 polymerase for 4 hours at 37 ^oC using B2 61-182 DNA template containing the T7 promoter (Table A.2)

2.1.6 Ligation

The creation of full-length B2 RNA containing inosine edits required ligation of the IVT product of the B2 61-182 sequence (Table A.2). To maintain proper control samples both the inosine modified synthesised RNA, as well as a control sample, were synthesised for ligation. These ligations were performed using RNA Ligase (New England Biolabs) and a DNA splint (IDT). The 3’ gBlock B2 RNA was treated with 1 µL PNK (10,000 U/ml), for 1 hour at 37 ^oC, followed by deactivation of the PNK enzyme at 65 ^oC for 20 minutes. After preparation of the 3’ RNA sequence, the DNA splint was hybridized to the RNA by heating the sample to 90 ^oC and then

slowly cooling it in a thermocycler at a rate of 0.1 ^{o}C per second until it has reached 25 ^{o}C. Following hybridization, 0.5 µL of RNA Ligase (30,000 units/ml) was added and allowed to incubate at 37 ^{o}C for 4 hours, followed by a further incubation step at room temperature for 16 hours. The samples were gel purified before being prepared for HSF-1 Processing.

2.1.7 HSF-1 Processing

Following ligation, the newly created B2 RNA transcripts (modified and control) are prepared for HSF-1 Processing. From each B2 RNA sample, 30 ng was taken and refolded in the thermoblock (Biorad) with the addition of 0.8 µL F2 buffer (300 mM NaCl, 50 mM Hepes) and H20 up to 4 µL. Each sample was heated to 50 ^{o}C for 1 minute followed by a decrease of temperature by 4 ^{o}C at a rate of 1 ^{o}C every 10 s. The refolded samples were split into two categories a control group for each sample type and a sample containing HSF-1 before incubation. To the HSF-1 group 0.5 µL H2O and 0.5 µL HSF-1 (7.8 nM) (Dissolved in TAP Buffer) were added, while the control group followed the addition of 0.5 µL of H2O and 0.5 µL TAP Buffer (5 nM Tris pH 7.9, 0.5 mM $MgCl_2$, 0.02 mM EDTA, 0.01% NP-40, 1% glycerol, 0.2 mM DTT). Both groups were incubated at 37 ^{o}C for 30 minutes.

2.2 Cell-Culture

2.2.1 Cell Line/Handling (HT22)

For all experiments, the cell line used was HT22 mouse hippocampal neuronal cells (Sigma). The cells were cultured in SG-22-expansion media containing High Glucose Dulbecco's Eagle Medium (Sigma) consisting of 1% L-Glutamine (Gibco) and 10% Fetal Calf Serum (Sigma). The cells were grown at 37 ^{o}C in an incubator with 5% CO_2. The cell culture plates were split when

considered fully grown, at about 70% confluence. To continue expansion to workable cell counts, from each flask the media was removed from flask bound cells by use of a vacuum pipette. The cells were rinsed of old media using phosphate-buffered saline (PBS) (Sigma) removed by a vacuum pipette. The flask-bound cells were removed from the flask by trypsinization using TrypLE Express (Gibco) and transferred to a falcon tube for pelleting by centrifugation. The pelleted cells were decanted by vacuum and resuspended in 10 mL of new media for each cell flask the cells are to be split into, before adding to flasks for expansion. When starting new experiments, HT-22 stocks were removed from liquid nitrogen and allowed to acclimate to 37 ^{o}C in a bead bath. Following climatization, the cells are added to 9 mL of expansion media and pelleted using centrifugation to remove the freezing media. The pelleted cells were resuspended in 10 mL of SG-22 expansion media and added into new expansion flasks. The creation of HT-22 Stocks was performed by following the splitting procedure and pelleting individual flasks followed by resuspending cells in 1 mL of media supplemented with 10% dimethyl sulfoxide (DMSO) (Sigma) in liquid nitrogen grade microcentrifuge tubes. The resuspended cells were placed at -80 ^{o}C for 24 hours before long term storage in liquid nitrogen.

2.2.2 Cell Counting

To facilitate, accuracy and consistency for experiments cells were counted before plating into flasks using a bright line hemacytometer (Hausser Scientific). Flasks of Cells were resuspended in 10 mL of media by trypsinization using TrypLE Express (Gibco) as previously outlined. A 20 µL sample from each plate is taken and placed on the bright line hemacytometer using light microscopy each of the 4 quadrants is counted for cells. The cell counts for each

quadrant were averaged and multiplied by ten to give an approximation of the cell count per microlitre for each flask.

2.2.3 Collection of RNA Sample for further RNA Assays

At the end of incubation, cells were sacrificed for harvesting genetic material (RNA). SG-22 expansion media was removed by vacuum, and the flask-bound cells were rinsed with 1 mL of PBS to remove previously dead cells and remove old media. The remaining cells were trypsinized using TrypLE Express (Gibco) to detach the cells from the flask before being transferred to a falcon tube using a pipette. The cells were then pelleted by use of a centrifuge and the remaining TrypLE is decanted off using a vacuum. The cell pellet is resuspended in 1 mL of Trizol and incubated for 5 min at room temperature, before being vortexed, and stored at -80 ^{o}C for 24 hours before being prepared for cDNA preparation.

2.3 Cell Culture Knock Down Assays

2.3.1 ADAR3 siRNA knockdown assay

Two hundred thousand cells were plated to each well of a 6-well plate and were acclimated at 37 ^{o}C for 24 hours. The expansion media was removed from each well by vacuum and the cells and washed with 1 mL of PBS, followed by the addition of 1.5 mL of expansion media with the siRNA samples containing 1.5 µL of ADAR3 siRNA TriFECTa DsiRNA Kit hs.Ri.ADARB2.13 (50 µM) (IDT) which contains a combination of three ADAR3 targeted siRNAs. The cells were incubated for 24 hours at 37 ^{o}C, and the addition of 287 mM final concentration of Glutamate was added and incubated for 30 minutes at 37 ^{o}C. After the incubation time, the cells were sacrificed and prepared for cDNA preparation.

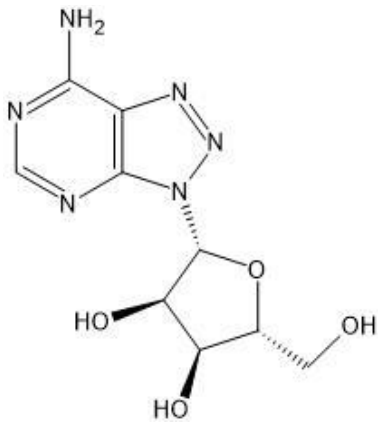

Figure 2.2: 8-azaAdenosine small molecule inhibitor of the ADAR family of enzymes. Figure created by ACD/ChemSketch FreeWare.

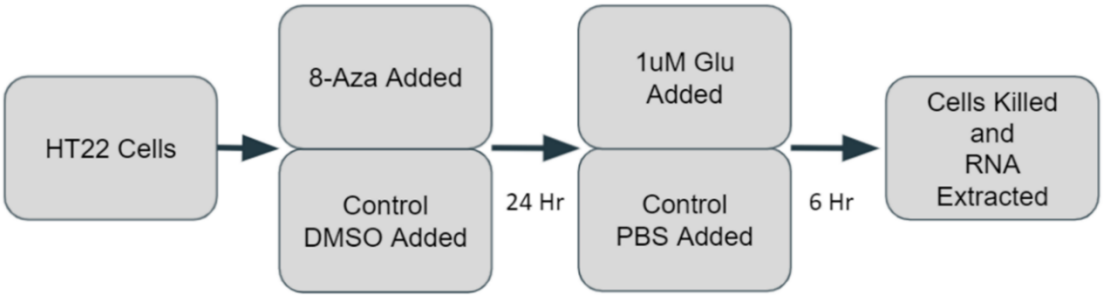

Figure 2.3: Experimental Design of HT22 cell line experiment using 8-azaAdenosine small molecule inhibitor with 1uM Glu cellular stress.

2.3.2 Small Molecule Inhibitor assay

In collaboration with Luke Saville, the HT22 cell line experiment was performed as portrayed in Figure 2.3, one million cells were plated into T75 cell flasks and acclimated at 37 ^{o}C for 24 hours. Media was removed by vacuum and the cells were washed with 2.5 mL of PBS, the cells were then resuspended in 5 mL of media containing 1 µM final concentration of 8-azaAdenosine small molecule inhibitor dissolved in DMSO (Fisher) (Figure 2.2) (100 µM). To the control flasks, DMSO of equal volume was added to the media. The cells were incubated for 24

hours at 37 ^{o}C, before the addition of 287 mM final concentration of Glutamate being added during the 24 hours and incubated for 6 hours at 37 ^{o}C. Following incubation, the cells were sacrificed and prepared for cell RNA Extraction for use in qPCR cDNA preparation.

2.4 Gene Expression Studies

2.4.1 RNA extraction

Previously frozen and sacrificed cells dissolved in Trizol were thawed in a 37 ^{o}C bead bath before being vortexed. To each sample 0.2 mL of chloroform per mL of media is added. After the addition of chloroform, the tubes were inverted and incubated for 2 minutes at room temperature, followed by centrifugation for 15 minutes at 4 ^{o}C, 12,000 g. The upper aqueous layer was transferred to a microcentrifuge tube with the addition of 500 µL of isopropanol (Fisher) and incubated at -20 ^{o}C for 30 minutes before centrifugation forming a pellet. The pellet was washed twice with 1 mL of 75% ethanol, before air drying and re-dissolved in 40 µL RNase free water, and stored at -80 ^{o}C.

2.4.2 Preparation of cDNA for use in qPCR

Extracted RNA samples were used to synthesize cDNA using SuperScript III first strand synthesis (Life Technologies) and 100 ng of random primers (New England Biolabs) using standard manufacturer protocols. Quantitative Polymerase Chain Reaction (qPCR) was performed using Luna qPCR Master Mix (New England Biolabs) and manufacturer protocols. Primer sequences (Table A.3). The reaction was performed using a thermocycler with the following conditions: 95 ^{o}C for 3 minutes, followed by 40 denaturation cycles of 95 ^{o}C for 15 s, annealing at 54 ^{o}C for the 30 s, and extension at 66 ^{o}C for 30 s.

2.5 Gel Electrophoresis

2.5.1 Urea PAGE

RNA samples were visualized and separated by size using 10% Urea PAGE gels. The creation of Urea PAGE gels was performed using a solution of 0.6 mL 5x TBE, 1.5 mL 40% acrylamide, and 3.3 mL H20, with the addition of 2.88 g of urea used to assist in denaturing the RNA. The polymerization of the gel was performed using 25 µL 10% ammonium persulfate (APS) and 5 µL tetrametthylethylenediamine (TEMED). Samples were loaded onto the polymerized gel and run for 60 minutes at 180 V in 1x TBE buffer solution. The gels were stained with SYBR Green II (Invitrogen) dye and scanned at the appropriate filters and wavelengths for the dye used (495nm).

2.6 In Vitro Synthesis of RNA for use in RNA Ligations of Full-length B2 RNA

2.6.1 Template Preparation through PCR

The Polymerase Chain Reaction (PCR) was performed using a 10 µL Q5 Reaction Buffer (5x), 1 µL dNTPs, 1 µL T7 promoter (20mM), 1 µL Reverse primer (20mM), 1 µL DNA Template (1:10 gBlock Stock) (IDT), and 35.5 µL H2O. The PCR mix was heated up to 98 ^{o}C before the addition of 0.5 µL of Q5 DNA polymerase, and mixed, before being added to the thermocycler under the following conditions: 35 cycles of (98 ^{o}C – 5 s, 58 ^{o}C – 10 s, 72 ^{o}C – 10 s), followed by 72 ^{o}C for 10 minutes, and stored at -20 ^{o}C.

2.6.2 T7 RNA PCR amplification

B2 DNA gBlock Sequence:

5’TAATACGACTCACTATAGTCAAATCCCAGCAACCACATGGTGGCTCACAACCATCCGTAACGAGATCT
GACTCCCTCTTCTGGAGTGTCTGAAGACAGCTACAGTGTACTTACATATAATAAATAAATAAATCTTTAA
AA 3’

The DNA template was produced from a gBlock (IDT) by PCR amplification using the T7 promoter, forward primer (T7): 5’-TAATACGACTCACTATAG-3’ and the reverse primer (B2) 5’-TTTTTTTTTAAAGATTTATTTATTTATTATATGTAAGTACA-3’ (Table A.2).

2.7.1 Data Analysis

Statistical analysis of qPCR data used a combination of paired and unpaired student’s t-tests to determine if the differences observed in qPCR relative expression were statistically significant. Furthermore, analysis of HSF-1 processing was analysis by 10% urea page gel densitometry in comparison to untreated controls to determine relative percent remaining of synthesized B2 SINE RNA. The percent remaining used paired student’s t-test to determine if the differences observed in remaining material were statistically significant.

Chapter 3

Results

3.1 Generation of Adenosine to Inosine modified B2 SINE RNAs through Solid-Phase RNA Synthesis

3.1.1 Rationale for the optimization of B2 SINE RNA solid-phase RNA synthesis

To investigate the impact of inosine modification on B2 RNA stability, the synthesis of B2 SINE RNA in vitro was required. However, to achieve this, optimization of the synthesis protocol was needed given the length of B2 RNA and the need to incorporate modified bases. In particular, in vitro transcription was employed to create B2 SINE RNAs containing modified bases. B2 SINE RNA containing modified RNA were created as shown in Figure A.1, and A.2; however, these RNAs were not suitable for studying the effects of RNA stability due to the presence in IVT products of some pre-processed gel bands following in vitro transcription. Moreover, the SINE RNAs generated through IVT were not representative of modified RNAs studied in vivo. During the in vitro transcription with Inosine, the latter replaces every guanosine within the B2 RNA sequence as Inosine binding affinities are like that of guanosine. In contrast, in vivo, modified B2 RNA modifications are targeted to specific adenosines within the B2 sequence. Due to these challenges with IVT, our approach switched to using Solid Phase RNA Synthesis on the K&A RNA/DNA Synthesizer, due to its ability to create base specific Inosine additions despite it initially having poorly optimized protocols for long-range (>40 bases) RNA synthesis, which we had to optimise (see the section below).

3.1.2 Development and optimization of the solid phase RNA synthesis protocols for modified B2 SINE RNAs

To create SINE RNA with specific RNA modifications, we used solid-phase RNA synthesis technology that is not prone to the shortcomings of IVT mentioned above. Our initial target was to generate full-length B2 SINE RNAs (> 180 nt) with the addition of specific Inosine modifications at specific positions. However, with current technology, Solid-Phase RNA synthesis is only optimized for the synthesis of RNA molecules in lengths of fewer than 40bp. Thus, the need for further optimization of currently available protocols was necessary to complete the synthesis of the desired full-length B2 RNA. Upon consultation with the manufacturer, coupling time was extended to 800 seconds from the 360 seconds typically used for RNA. The increased coupling time aimed to ensure step-by-step yield through the synthesis process for long sequences, and simultaneously provide additional time for modified bases (Inosine) with a lower efficiency to couple. With this initial optimization RNA amides including Inosine were reconstituted and 182 bp B2 sequences were synthesised with one sequence containing three Inosine additions (Figure 3.1) along with control B2 sequences (Figure3.2). Following this initial synthesis, the optimizations showed to be effective at maintaining the step-by-step yield throughout the synthesis by maintaining a 99.8% step by step yield in both sequences. However, the total yield of both sequences continued to be low over time with the “B2RNAI” and “B2RNA” sequences completing the synthesis run with total yields of 74% and 63%, respectively. Despite, the B2RNAI sequence completing the synthesis run with a higher total yield, the possibility of base coupling omissions caused by the addition of Inosine bases could generate a sequence bias with undesired deletions. An indication of deletion events occurring during coupling reactions can be seen during

the synthesis of the first inosine base at position 46 where the following base results in a total yield of 50% followed by the subsequent base at recovering to 65%. Therefore, the increase in yield from one base to another indicates a failure of the inosine to couple while the sequence continues to synthesize. From the preliminary results obtained it was clear that extending the capabilities of RNA solid-phase synthesis would provide a method for studying the effects that Adenosine to Inosine modification would have on the stability of full-length B2 RNA to fulfill the necessary for the aims laid out in this thesis.

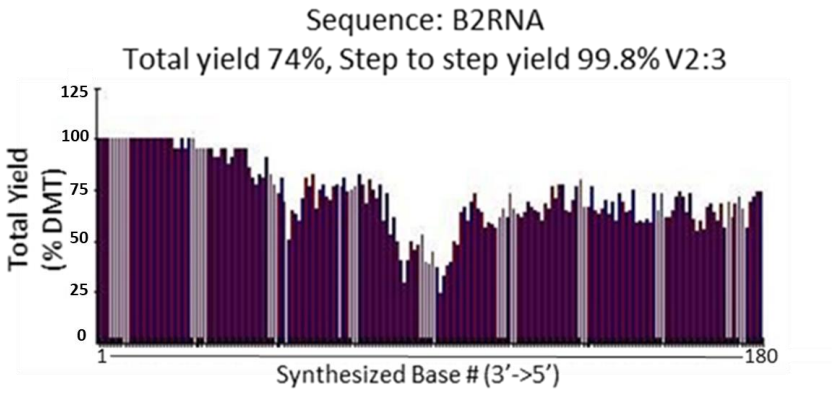

Figure 3.1: During the synthesis of the full 180 bp sequence B2 RNA shows a drop in total RNA yield overtime during synthesis of the "B2RNAI" sequence. Specifically around the addition of Inosine RNA bases. Calculated by the removal and detection of DMT- protecting group in comparison to the DMT released by the previous base by percentage. B2RNAI sequence representing 180bp containing the addition of three inosine modifications. Throughout synthesizing 180 bp overall synthesis using the K&A synthesizer shows an overall reduction of total efficiency. Base numbers at the x-axis represent 3'-5' direction. Inosine additions at position 91, 111, and 134.

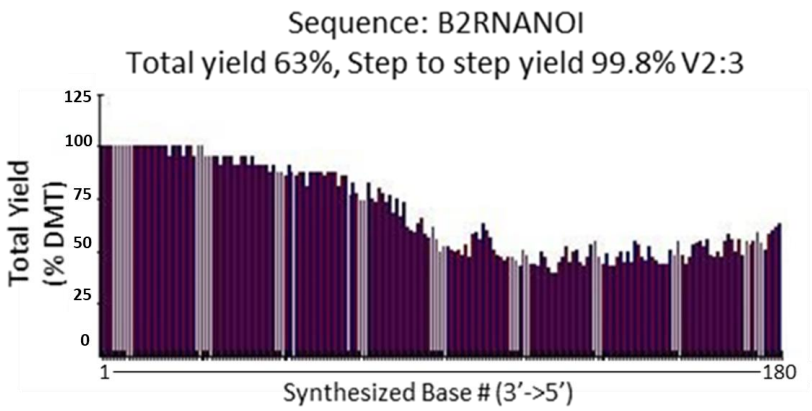

Figure 3.2: RNA Synthesis of the full B2 RNA still shows a drop in total RNA yield over time on the synthesis of the control "B2RNA" sequence. Calculated by the removal and detection of DMT-protecting group in comparison to the DMT released by the previous base by percentage. B2RNA sequence representing 180bp. Throughout synthesizing 180 bp overall synthesis using the K&A synthesizer shows an overall reduction of total efficiency. Base numbers at the x-axis represent the 3'-5' direction.

3.1.3 Modification of the SINE B2 RNA synthesis length, along with changes to reagent temperature conditions lead to optimizations of solid-phase synthesis

To further improve synthesis, several optimizations were made after initial synthesis attempts to limit the potential loss of important modified bases. The first intervention was to mitigate the reduction in overall yield during synthesis that results from the step-by-step yield from each base that is synthesized. To this end, synthesis of slightly shorter RNA sequences was attempted, and the first candidate for this was a 100bp "100BPOZ" sequence created for testing the 100bp sequences (Table A.1). Although a length of 100bp would fail to produce full-length B2 RNA, it would be an improvement on the typically synthesized lengths of 20-40 base pairs.

Nevertheless, the synthesis of the "100BPOZ" sequence in Figure 3.3 resulted in a reduction in synthesis efficiency with a total yield of 32%. This reduction of total yield over Figures

3.1 and 3.2 points to a loss in the efficacy of the reconstituted amides, as they were stored at room temperature while attached to the RNA synthesizer during the synthesis of the previously mentioned sequences. The storage conditions of amides (the four RNA bases and Inosine base modified for synthesis) are often overlooked while on a synthesizer as during DNA synthesis each base takes approximately one minute to synthesize while our long-range synthesis requires around sixteen minutes per base. To account for this loss of efficacy due to storage conditions, we lowered the temperature of the amides with the application of external cooling during synthesis. This results in the reduction of the temperature in which the amides are exposed to while attached to the RNA synthesizer which are used for the synthesis of new B2 SINE RNA along with fresh amides to ensure efficacy.

Subsequently, the B2 SINE RNA sequence was split into two fragments the 3' end (100bp) (Sequence B2CT4EN4) (Figure 3.4) and the 5' end (80bp) (Sequence B2CT5END) (Figure 3.5). The changes in storage temperature and the introduction of fresh amides resulted in total yields of 66% and 63%, respectively, and reduced the occurrence of base recovery caused by a base failing to couple for a single round of synthesis, as seen by the recovery of total yield in Figure 3.1.

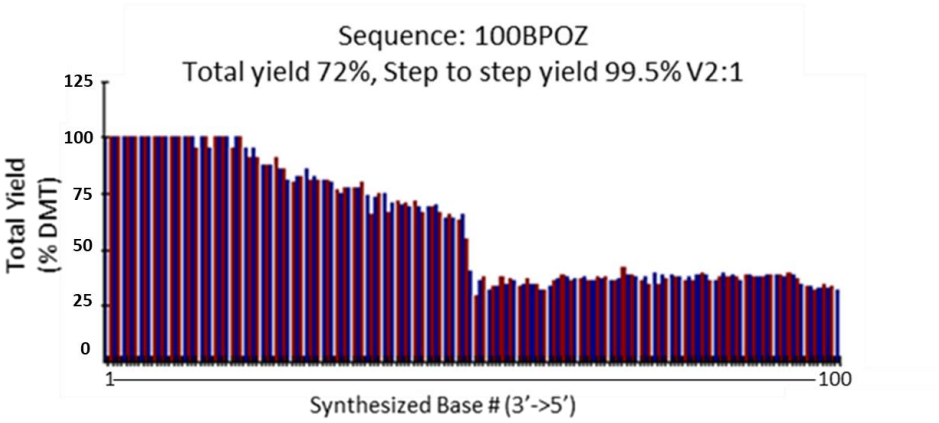

Figure 3.3: Reduction of B2 RNA synthesis limited to 100bp shows lose of total RNA yield half way through synthesis of the "100BPOZ" sequence. Calculated by the removal and detection of DMT-protecting group in comparison to the DMT released by the previous base by percentage. 100BPOZ sequence represents a 100 bp sequence designed to help test and optimize long RNA synthesis. Throughout synthesizing 100 bp overall synthesis using the K&A synthesizer shows an overall reduction of total efficiency. Base numbers represent the 3' – 5' direction.

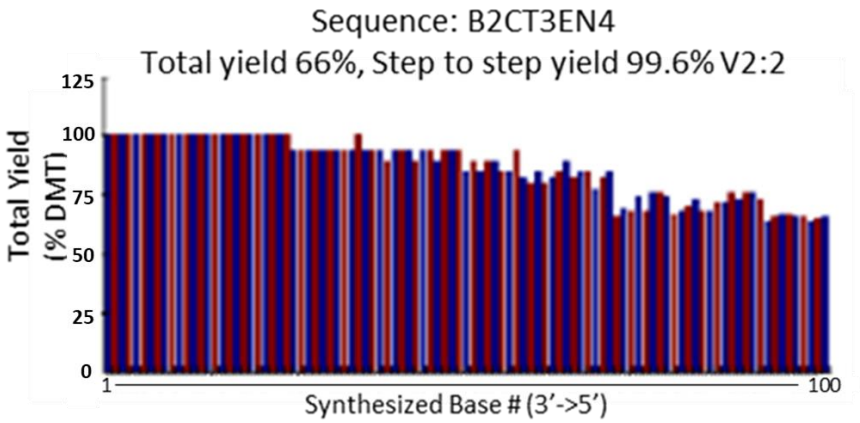

Figure 3.4: A reduction in RNA amide storage temperatures improve the overall RNA Synthesis total yield along with a reduction in single base pair deletions during the synthesis of the "B2CT3EN4" sequence. Calculated by the removal and detection of DMT- protecting group in comparison to the DMT released by the previous base by percentage. B2CT3EN4 sequence represents the 100bp found on the 3'end of the B2 SINE RNA. Base numbers at the x-axis represent 3'-5' direction.

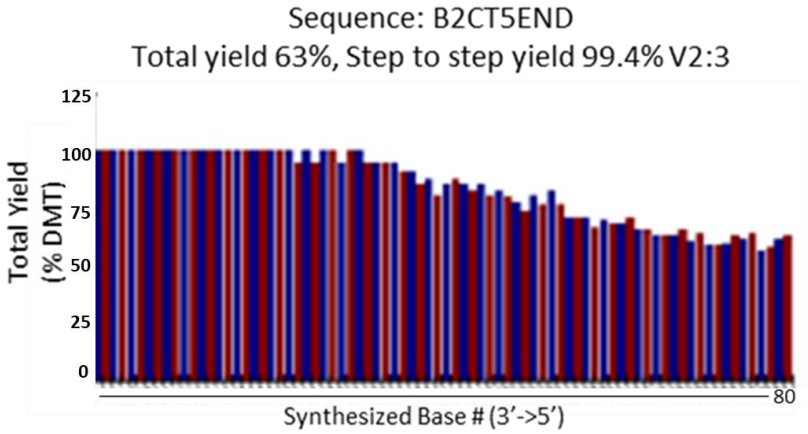

Figure 3.5 RNA Synthesis of the 80bp 5' end of the B2 RNA shows an increase in total yield along with a reduction in recovered bases resulting in a decrease of potential deletions during the synthesis of the "B2CT5END" sequence. Calculated by the removal and detection of DMT-protecting group in comparison to the DMT released by the previous base by percentage. B2CT5END sequence represents the 80bp found on the 5'end of the B2 SINE RNA. Base numbers at the x-axis represent the 3'-5' direction.

3.1.4 Purification and ligation of B2 SINE RNA 5' and 3' synthesised fragments

To create full-length SINE B2 for HSF-1 stability assays, ligation of the 5'-end and 3'-end synthesized fragments is required. Therefore, following the extraction and deprotection (Section 2.13) of the "B2CT3EN4" and "B2CT5END" fragments, both B2 RNA fragments required further purification (Section 2.14). In Figure 3.6 both the 5' end and 3' end fragments are visualized showing multiple RNA bands because of the gradually decreasing synthesis yield over time truncated products that form as a result. However, unexpectedly, the 5'-end fragment resulted in a faint band at the 80 BP band, while the relatively darker band was found for the full length 3' end at the 100BP band. This may have been a result of losses of yield during synthesis and deprotection or due to the ribozyme activity of the B2 SINE RNA. Despite, the reduced recovery of this fragment, we performed ligation alongside a DNA splint to ensure directionality and to

ensure ligation of only full length 3’ end fragments. The ligation of the 100 bp and 80 bp 3’ and 5’ ends B2 SINE RNA (Figure 3.7) failed to produce a full-length sequence, requiring us to look at further optimizations and potential issues within the previously established protocols.

Firstly, a determination had to be made as to if either the product or the components of ligation were stable throughout the entire ligation procedure. The ribozyme activity of the B2 SINE RNA may be responsible for degrading the RNA when exposed to the increased temperatures of ligations during the 37 ^{o}C incubation time along with potential ribozyme activities of the fragments themselves during PNK 65 ^{o}C incubation, and the 90 ^{o}C hybridization of the DNA splint. To address these concerns, a modified ligation protocol that uses a reduction of the 37 ^{o}C ligation period was used extending the ligation time from 4 hours at 37 ^{o}C ligation to 1-hour at 37 ^{o}C followed by 20 hours at room temperature. Secondly, the reduced quantity of the 5’-end fragments may have been problematic to overall ligation as the reduced yield may already be expected due to ribozyme activity, thus, the alternative sequence with a smaller length may provide an improved yield as they may allow for efficient ligation resulting in increased recovery of RNA post-ligation.

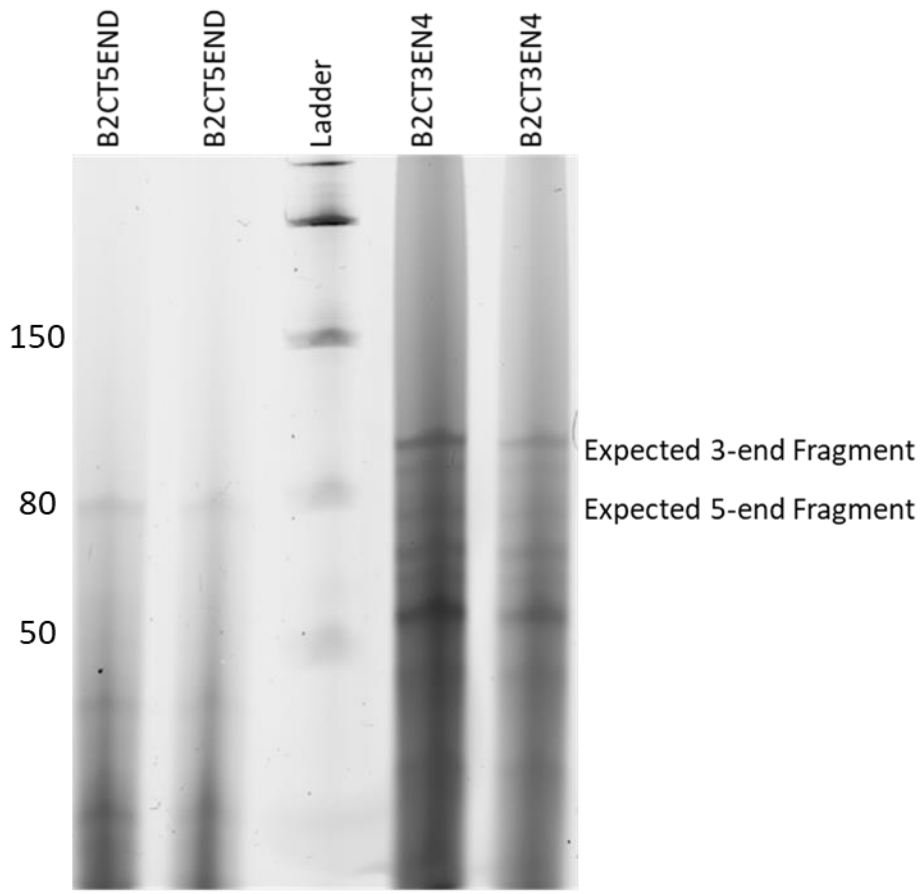

Figure 3.6: 10% Urea-PAGE of synthesized B2 fragments, extracted and deprotected following RNA solid-phase synthesis. Each lane represents 5 microlitres of deprotected synthesized RNA. From each lane, the gel was extracted at the 80bp (5'end) and 100 bp size bands. Each fragment gel extracted was used for further purification of the ligations of full-length fragments.

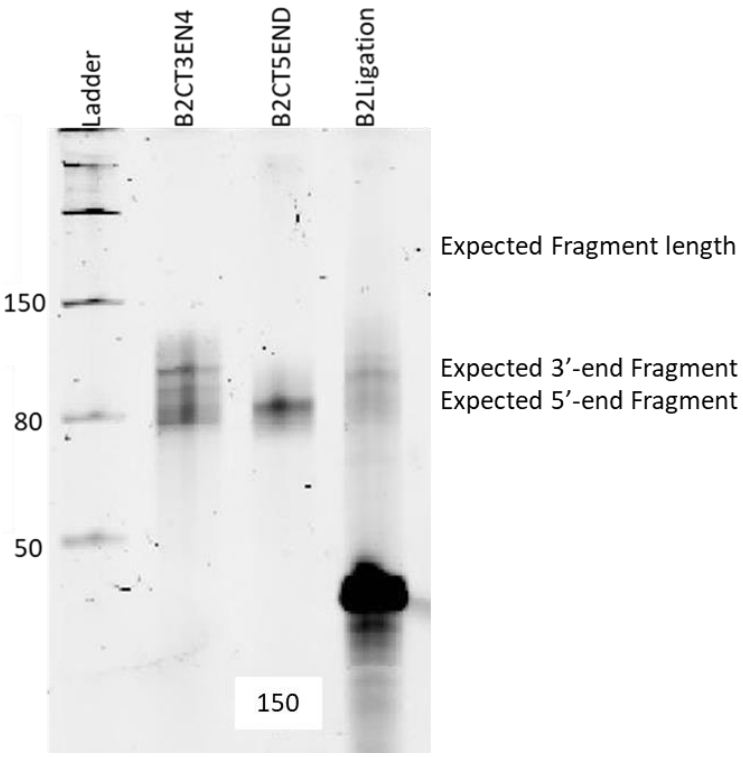

Figure 3.7: 10% Urea-PAGE of purified synthesized B2 fragments and their RNA ligation alongside a DNA primer. Each lane represents 1 microlitre of purified B2 fragments, and a combined 2 microlitres are found in the ligation. Ligation results in the overall processing of the 5'-end sequence in the final ligation.

3.1.5 Addition of modified Inosine during RNA solid-phase synthesis results in a step-by-step and total yield drop

To study the effects of the addition of modified inosine during solid-phase synthesis, inosine amides were added in addition to the four canonical RNA bases to the synthesizer. Synthesis of the B21-60I RNA sequence containing three specific inosine locations as decided based on data about potential editing locations acquired through collaboration with Liam Mitchell to determine the location of *in vivo* inosine sites (Figure 1.2). Synthesis of the B21-60I sequence resulted in a total yield of 52% while it showed several losses in total yield during inosine base addition occurring at following directly following the addition of the first Inosine at

position 12 and directly during the synthesis of the second Inosine at position 29 (Figure 3.8) because of the reduced synthesis efficiency, alongside reductions in step-by-step yield occurring at position 24 and 32. Furthermore, following the base additions we saw a recovery in overall efficiency pointing to a potential deletion of the inosine base from the RNA. In contrast Figure 3.9 shows the synthesis of the control B21-60 RNA sequence (no Inosine) which shows a consistent descending yield throughout the 60 base pair sequence. This slow stepdown reduces the probability of deletions while resulting in a total yield of 45%.

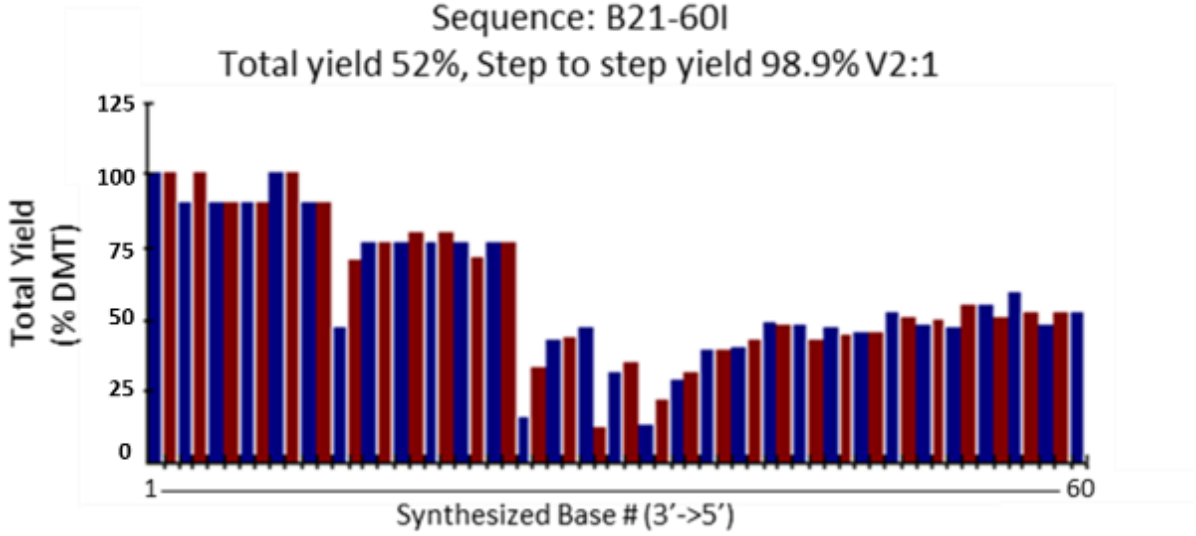

Figure 3.8: Synthesis of the RNA sequence B21-60I containing inosine modifications shows a drop in step-to-step yield during bases containing the inosine. Calculated by the removal and detection of DMT- protecting group in comparison to the DMT released by the previous base by percentage. B21-60I sequence contains the first 60 base pairs of the B2 sequence with Inosine replacing the adenosine at position 26 (P34), position 31(p 29) position 49 (p 11), position results in loss of overall synthesis efficiency and total yield. Base number represents 3'-5' direction.

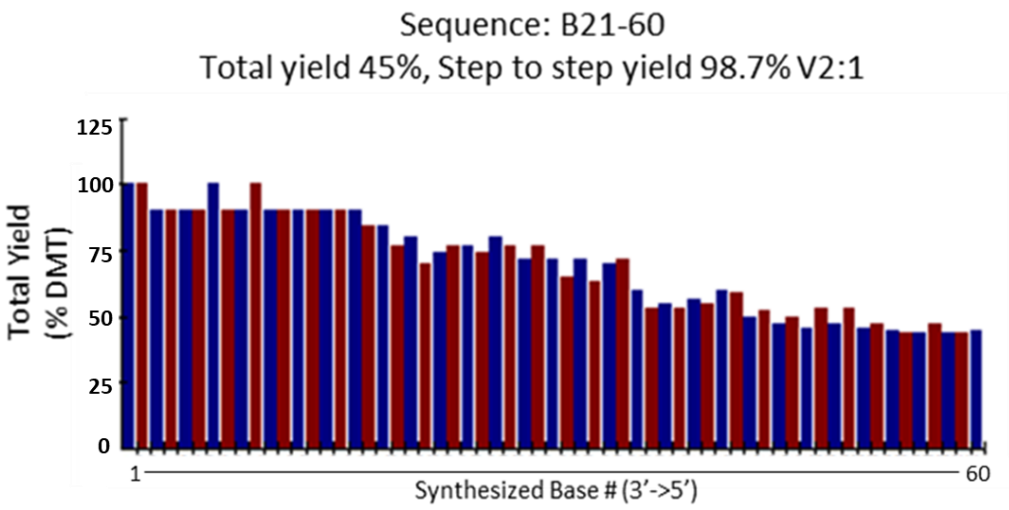

Figure 3.9: RNA Synthesis shows a standard reduction in total yield throughout synthesis, during synthesis of control B21-60 sequence. Calculated by the removal and detection of DMT-protecting group in comparison to the DMT released by the previous base by percentage. Synthesized with Sequence B21-60 Base number represents 3'-5' direction

3.1.6 Addition of a single modified RNA inosine results in a smaller drop in yield.

To increase the efficiency of synthesis the decision to include only a single inosine nucleotide in each sequence was made to improve overall yield. Figure 3.10 shows the addition of the inosine bases results in a reduction in overall yield to 50% immediately following the addition at positions 12 and 13, although the following bases maintain a high total yield for the rest of the synthesis resulting in a total yield 81%. With a total yield of 81%, we would be able to infer that the extracted RNA would not contain the inosine edits due to the yield of inosine sitting at only 50% leading to a fraction of the RNA having the inosine base as a deletion. For the ability to have success with these sequences for further experiments a higher efficiency of incorporating inosines would be required. Therefore, further optimization is required to improve the yield of inosine base additions, resulting in the addition of a sacrificial sequence that contains a random

assortment of bases with an Inosine occurring one base before that of the sequence of interest to prime the inosine into the synthesizer to increase overall efficiency.

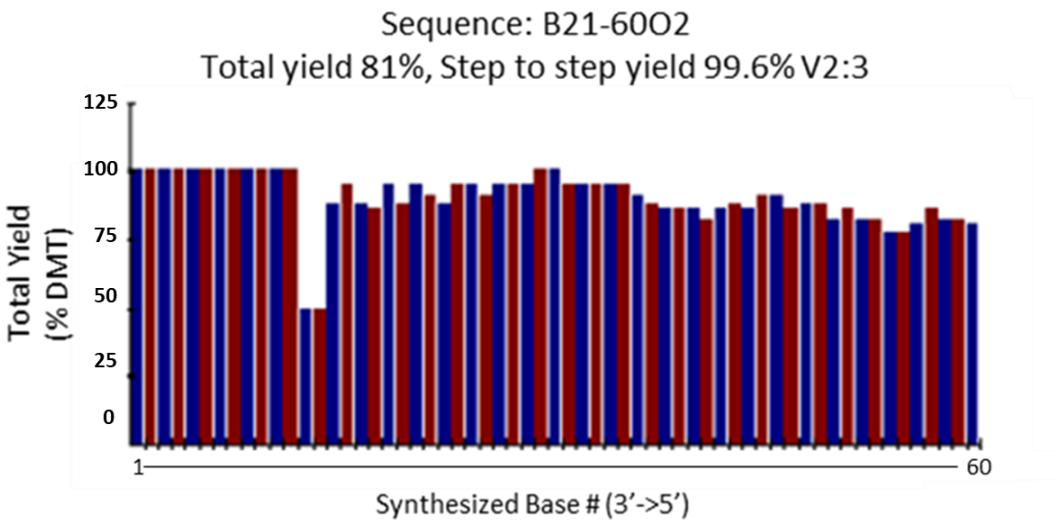

Figure 3.10: Addition of a single inosine in the sequence B21-60O2 sequence shows recovery immediately following its addition leading to the potential for deletions of the Position 49 of the sequence. Calculated by the removal and detection of DMT- protecting group in comparison to the DMT released by the previous base by percentage. B21-60O2 sequence contains the first 60 base pairs of the B2 sequence with Inosine replacing the adenosine at position 49 (position 11) resulting in loss of overall synthesis efficiency and total yield followed by recovery overall. Base number represents 3'-5' direction.

3.1.7 Priming of the RNA solid-phase synthesizer results in further optimization and an increase in overall yield.

To improve the overall yield of inosine additions, priming of the device, far beyond the one recommended by the manufacturer was applied. In detail, a "sacrificial" sequence was created to run alongside the standard sequence that included an inosine addition as a single base before that of the sequence of interest. The addition of the "sacrificial" sequence resulted in a physical synthesis optimization due to the K&A H-8 synthesizer's reliance on argon compressed

capillaries to move the amides, this additional priming step allows for the inosine base to be used immediately before its addition. The addition of the "sacrificial" sequence (Figure 3.11) resulted in a slightly reduced total yield of 72% but the inosine base at position 12 showed an increase in coupling efficiency with a total yield of around 73%. Furthermore, the lower overall recovery following the addition of inosine to 85% shows a reduction in the number of potential deletions occurring at that base. Therefore, Figure 3.11 shows that the priming of the synthesizer and specifically that of inosines can dramatically improve modified RNA nucleotides synthesis efficiency for modified RNA bases. With the successful addition of a "sacrificial" sequence, we were able to limit the possible deletions which occur within the sequence due to coupling. Therefore, with this sequence, we were able to progress to the creation of full-length B2 modified SINE RNA by ligation, necessary to fulfil the aims of this thesis.

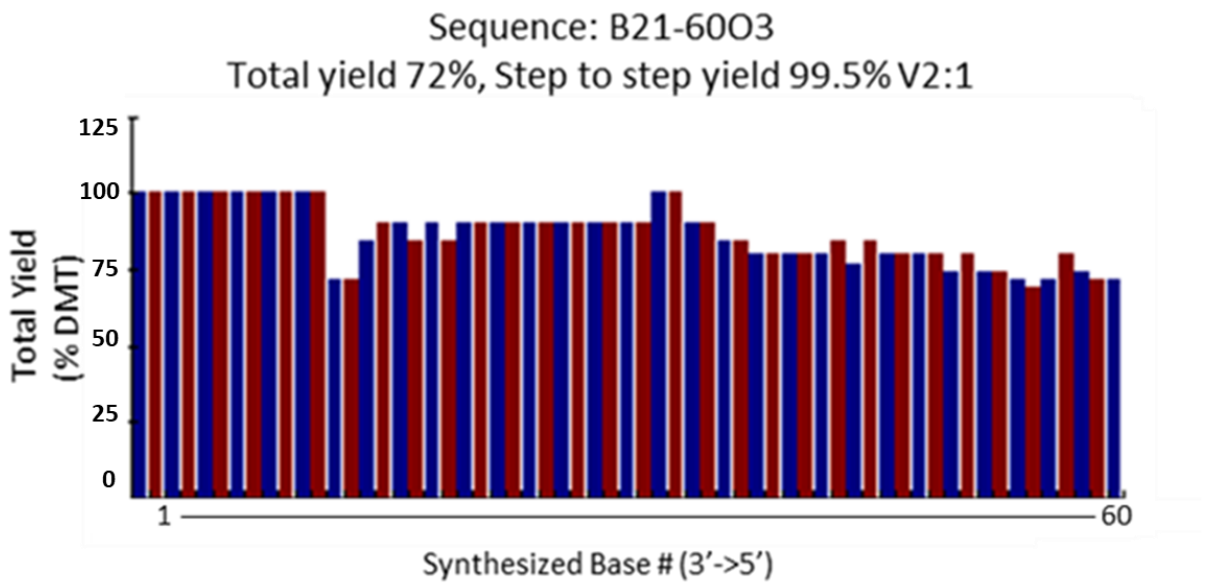

Figure 3.11: Synthesis of the B21-60O3 (B21-60O) sequence shows a successful synthesis of a total yield of 72% through the assistance and the addition of a sacrificial sequence. Calculated by the removal and detection of DMT- protecting group in comparison to the DMT released by the previous base by percentage. B21-60O3 sequence contains the first 60 base pairs of the B2 sequence with Inosine replacing the adenosine at position 49 (position 11) run alongside a sacrificial sequence containing the inosine base to prime the K&A synthesizer for use of the base resulting in a stronger step-by-step and total yield. Base number represents 3'-5' direction

3.1.8 Purification of successfully synthesized modified B2 RNA by RNA gel extraction.

In preparation for the ligation, the synthesized B2 RNA was Urea-PAGE gel-purified to eliminate the large range of non-specific synthesized RNA products as a result of deletions and loss of yield during synthesis. Figure 3.12 shows a 60bp RNA fragment which represents the full-length synthesized sequence. Furthermore, several degraded bands are also found within both the B261-122 and the B21-60I samples despite the gels being overloaded to ensure an adequate 60bp sample for purification. Following the gel purification, Figure 3.13 shows the B21-60I sample with three prominent bands in contrast to the initial synthesized samples. With the use of the UREA-PAGE gel purification, the B21-60I samples were clean enough to be used in ligation as

additional bands are a result of terminated sequences that are a resulted of failed base additions during synthesis and will be mitigated by the sequence specific ligation using the aforementioned DNA splint while the B261-122 resulted in an inadequate recovered quantity to be examined in the following purification, thus an alternative synthesis approach for the 61-182bp section had t*o* be considered for the creation of the ligated products (see next sect*ion)*.

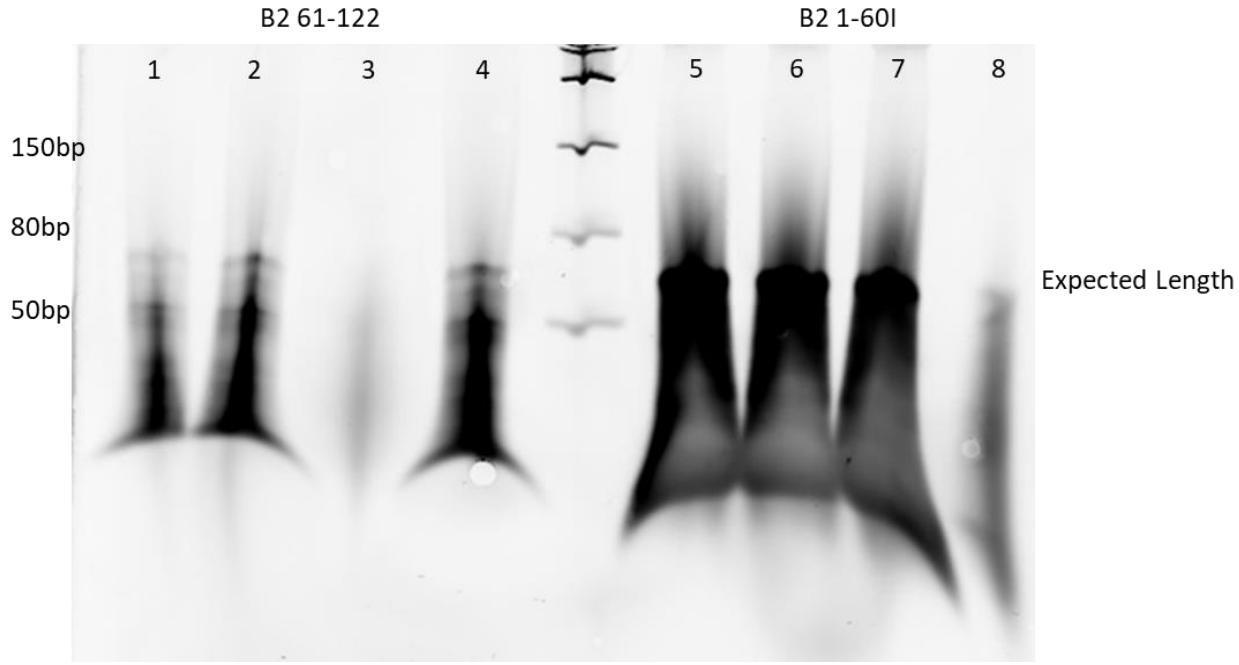

Figure 3.12: Urea-PAGE electrophoresis of synthesized B2 fragments, following purification and deprotection. Each lane represents 5 microlitres of final purified synthesized RNA (B2 61-122 - 40 µg/µL, B21-60I 100 µg/µL) with 60 bp fragment gel extracted for further purification of full-length fragments. Lanes 1-4 represent synthesized B2 bp 61-122, lanes 5-8 B2 1-60 represent synthesized B2 with Inosine addition at position 49.

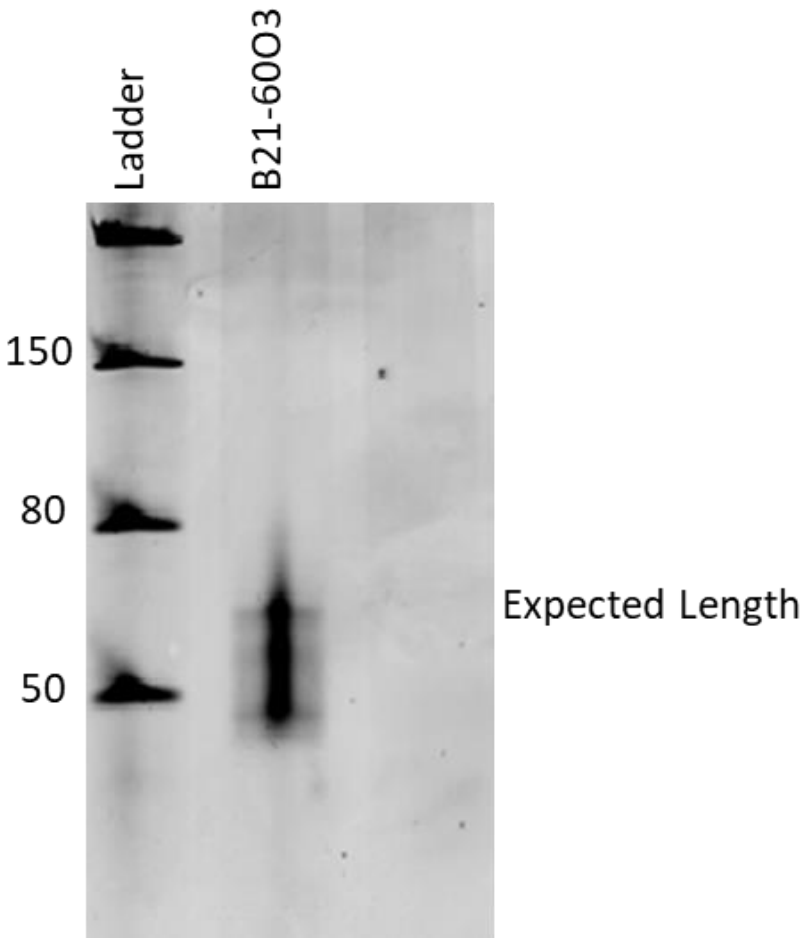

Figure 3.13: Urea-PAGE of gel extracted B21-60O3 RNA sequence after two rounds of gel-extraction representing 60ng of RNA. B2 with Inosine contains B2 Bp 1-60 with an inosine addition at position 49.

3.1.9 Ligation of the B21-60I RNA and IVT B2 SINE RNA (61-182bp) fragments

For the fragment for which we received a lower yield through the synthesizer (61-182bp), we employed standard IVT. Subsequently, to create full-length Inosine modified SINE B2 RNA from the B21-60I and an IVT B2 SINE RNA transcript(61-182bp) we optimized the standard RNA ligation protocol. In previous work the B2 has been known to have a level of ribozyme activity, thus during initial attempts to do ligation in two steps, it led to processing during the incubation process of RNA ligation. In contrast, we combined ligation and processing into one step to

prevent the self-cleaving of the second fragment prematurely during the ligation. Figure 3.14 shows the successful ligation of the two B2 SINE RNA both containing Inosine and the Control sequence at the expected length. Furthermore, it shows the effect of HSF-1 treatment on synthesized B2 SINE RNA resulting in processing.

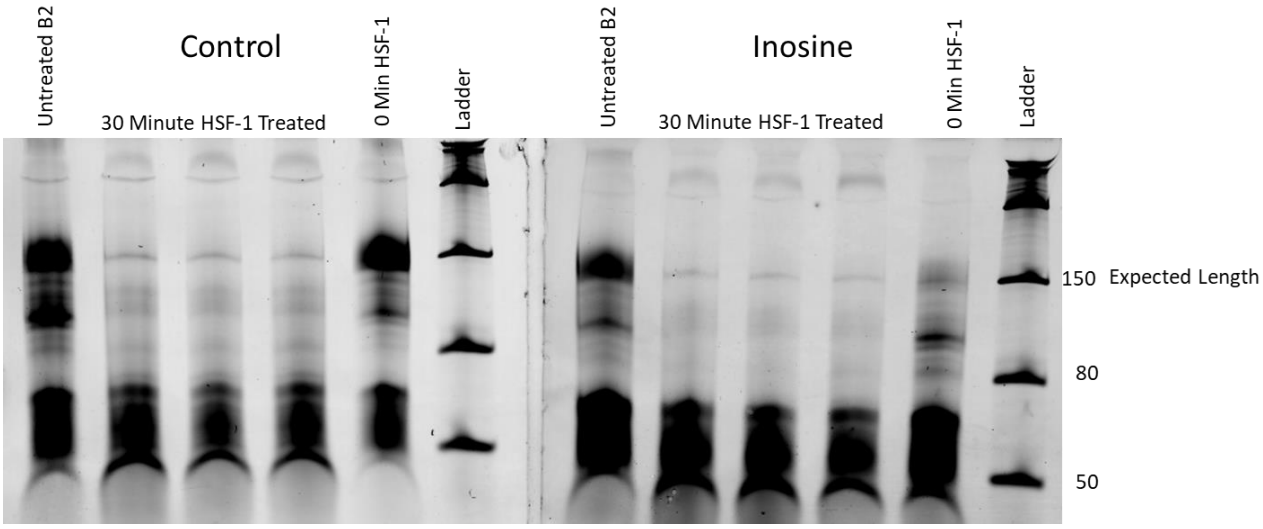

Figure 3.14: 10% Urea Page gel showing the ligation of the synthesized B2 RNA products (B21-60O3) with the IVT 61-181 B2 RNA product resulting in the expected B2 SINE RNA length. Alongside processing of the B2 RNA for 30 minutes with 7.8 nM HSF-1.

3.1.10 HSF-1 processing of modified B2 SINE RNAs

To determine the effects that the addition of inosine modifications has on the stability of B2 RNA, the ligated B2 RNA containing inosine of section 3.1.3 was incubated along with HSF-1 (previously shown to process B2). Changes in the HSF-1's ability to process the B2 SINE RNA has is measured as a direct relation to the stability of the RNA. To this end it has been excluded that the protein has RNA contamination through previous works (Cheng et al. 2021) to ensure the accuracy of the results. Therefore, the B2 SINE RNA was processed by HSF-1, for a total of 30 minutes. Figure 3.15 shows a significant reduction in processing rate where 14.6% of Inosine

modified B2 RNA remained following incubation with HSF-1, in contrast to the control, in which 3.7% remains following incubation. In conclusion, these results reveal that the presence of inosine at position 49 of the B2 SINE RNA results in a slower rate of processing when exposed to HSF-1. This confirms the hypothesized protective effect of Inosine edits on the B2 SINE RNA described in one of the aims of this thesis.

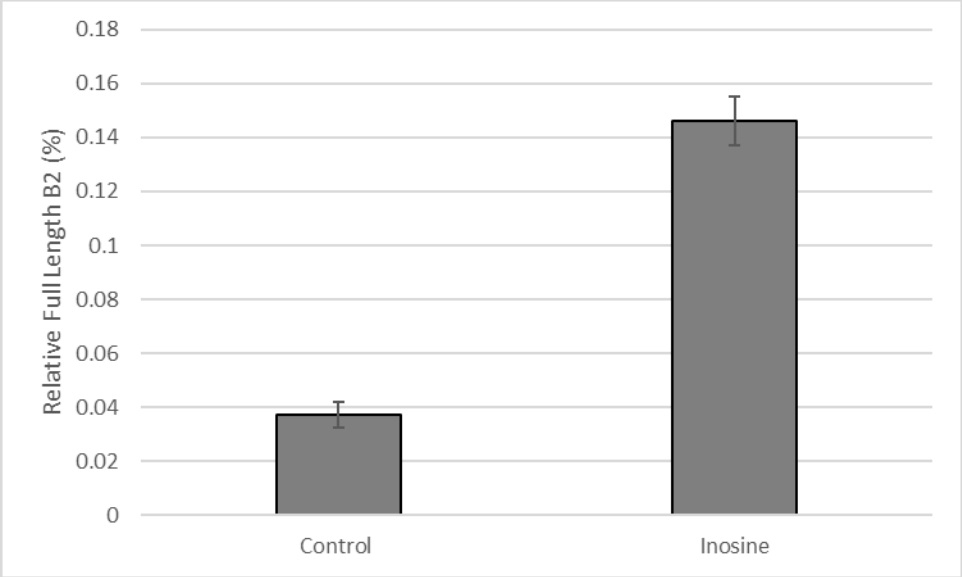

Figure 3.15: Relative Full-length B2 percentage remaining following 30-minute incubation with 7.8 nM HSF-1. B2 was refolded in a thermocycler before incubation. Full-length B2 was created by ligation of K&A synthesizer synthesized RNA B2 bp 1-60 with IVT gBlock B2 61-182. With the Inosine sample containing a modified Inosine base at position 49 in place of adenosine. Remaining percentage was determined by densitometry from 10% Urea PAGE gel (p=0.0005 paired t-test; CT-n=3; Inosine-n=3). *Relative Full-Length B2 calculated by comparison of B2 Full-Length band density as compared to incubated control samples.

3.2 ADARB2 siRNA Knockdown Assay

3.2.1 ADARB2 expression is tissue-specific and at lower levels compared to ADAR1

To determine the impact that the knockdown of the ADAR enzymes will have on total A to I editing rates, we investigated the overall expression levels of the ADAR enzymes, at the

tissue-specific level. ADARB2 is partly responsible for the control of adenosine to Inosine, due to being antagonistic to the ADAR1 enzyme. As shown in Figure 3.16, gene expression datasets minded from publicly available gene expression databases ADARB2 to be primarily transcribed within the cerebral cortex. In contrast Figure 3.17 shows that ADAR1 expression is prominent across a wide variety of tissues with the spleen and parathyroid gland having expression levels surpassing 150 transcripts per million reads. Due to the high expression levels of ADARB2 in brain tissue and the potential links that A to I editing may have on the stability of B2 SINE RNA, we hypothesized that the reduction of ADARB2 and subsequent increase in A to I editing may have a protective effect on the B2 RNA processing rates.

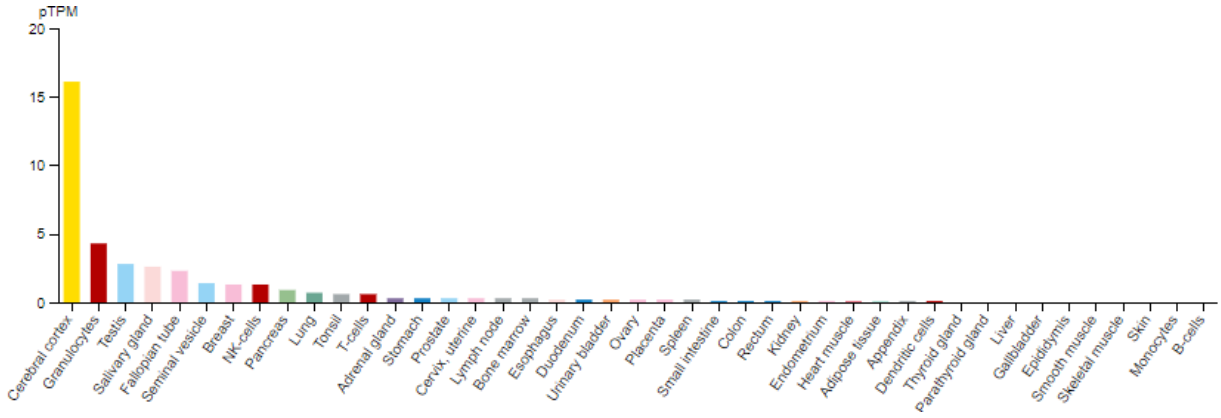

Figure 3.16: Tissue-specific ADARB2 transcripts per million reads produced by The Human Protein Atlas V.19 (July 2021), ADARB2 HPA dataset v19.proteinatlas.org (Uhlen et al. 2015)

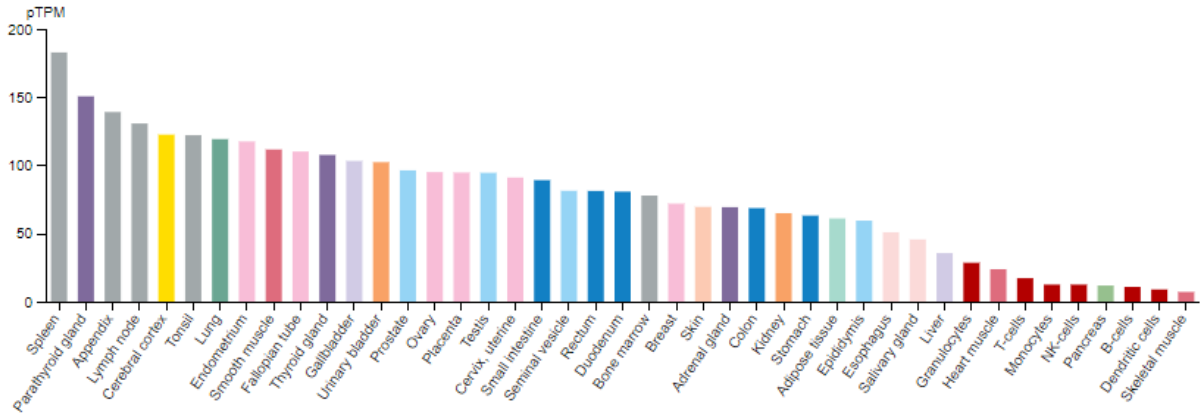

Figure 3.17: Tissue-specific ADAR1 transcripts per million reads produced by The Human Protein Atlas V.19 (July 2021), ADAR1 HPA dataset v19.proteinatlas.org (Uhlen et al. 2015)

3.2.2 The Downregulation of ADARB2 by anti-ADARB2 siRNA shows synergistic effects with Glutamate (GLU) toxicity

To study the effect that A to I editing has on the stability of B2 RNA, we applied a knockdown of ADARB2 using anti-ADARB2 siRNAs. Figure 3.18 shows that the addition of siRNA resulted in a reduction of ADARB2 transcripts expression, as assessed through qPCR. We then questioned whether the response to cellular stress would act synergistically with the ADARB2 KD. Indeed, as shown in Figure 3.18, the application of glutamate toxicity resulted in further reduction of ADARB2 expression. These results revealed that cellular stress affects ADARB2 levels. Because our main biological model is that of response to cellular stress, the above association would introduce a potential confounding factor in our analysis of the effect of A to I editing on B2 RNA stability, given that this is also affected by the cellular response to stress. Thus, we needed to find an alternative way to reduce editing without targeting the ADAR enzymes.

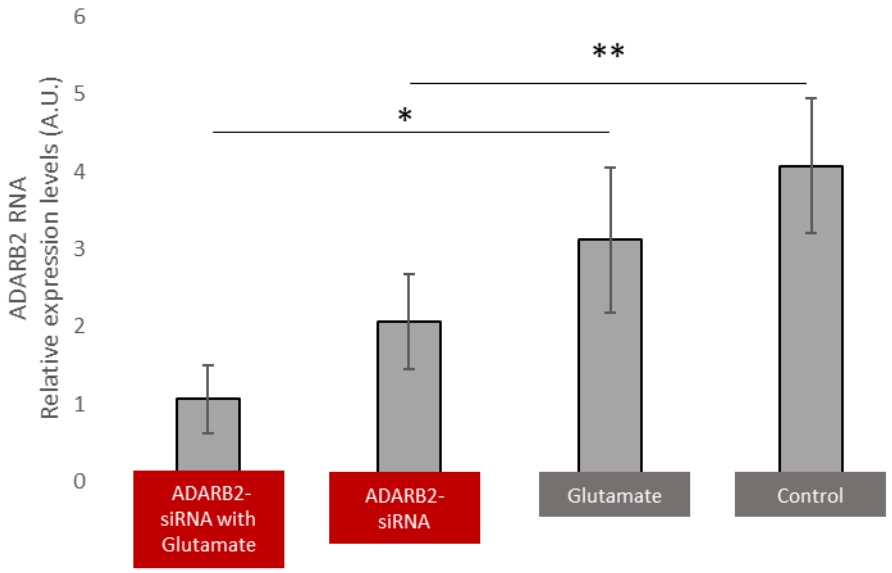

Figure 3.18: ADARB2 gene expression following incubation with anti-ADARB2 siRNA and glutamate cellular stress. Cells were HT22. Gene expression was determined using a relative standard curve of HPRT. The appropriate cells were incubated with a 4µM final concentration of siRNA for 24 hours followed by 1 hour with the addition of 1 µM of Glutamate. All steps were performed with cells at 37°C. Each group consisted of 4 plates of cells, with an outlier being excluded from Glu+. Represents the Mean value of the group n=4 (n= number of independent experiments) (* = p=0.01 unpaired t-test) (** = p= 0.0002 paired t-test).

3.3 8-azaAdensoine Small Molecule Inhibitor Assay

3.3.1 Reduction of Inosine editing by inhibition of ADAR1 by 8-AzaA shows a reduction in full-length B2 levels

We then questioned whether we could inhibit A to I editing activity in a way that does not include the KD of ADAR enzymes. To this end, we used the A to I editing inhibitor 8-azaA. The use of 8-azaA was chosen as a small molecule inhibitor for the effective inhibition of ADAR1 activity but not expression levels (Cat. No. 6868, Tocris). Expression of full-length B2 assessed through qPCR following incubation using 8-azaA along with glutamate toxicity shows a reduction in full-

length B2 RNA (Figure 3.19) confirming the results of our in vitro assays above that changes in Inosine editing plays a role in the processing of B2.

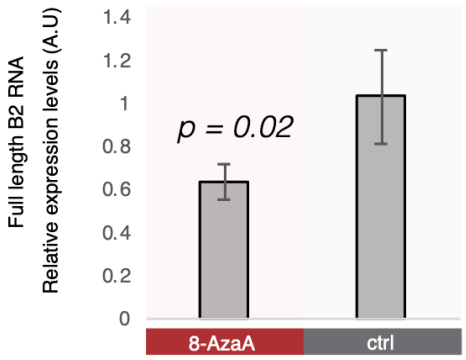

Figure 3.19: One-hour cellular stress HT-22 cells. Full-Length B2 RNA expression produced by qRT-PCR of A-to-I editing inhibited cells using Adar1 siRNA. The reduction of editing results in an overall destabilization of B2 RNA and an overall reduction in expression level. p=0.02 (unpaired non-directional t-test) n = 3, (n represents number of independent experiments) (Mitchell, Turner, et al, submitted).

3.3.2 Effect of 8 AzaA on B2 levels is observed only upon cellular stress

To determine if the impact of inhibiting A to I editing on B2 levels is independent of response to cellular stress, we repeated the sets of experiments of the previous section to include treatment with 8 AzaA also in the absence of cellular stress. Figure 3.20 shows that 8-AzaA when combined with cellular glutamate stress shows a significant reduction in overall full-length B2 RNA. In contrast, 8-AzaA shows no significant change over a control trial containing no glutamate toxicity. Thus, a reduction in overall inosine editing is correlated with a direct change in full-length B2 expression only in response to cellular stress.

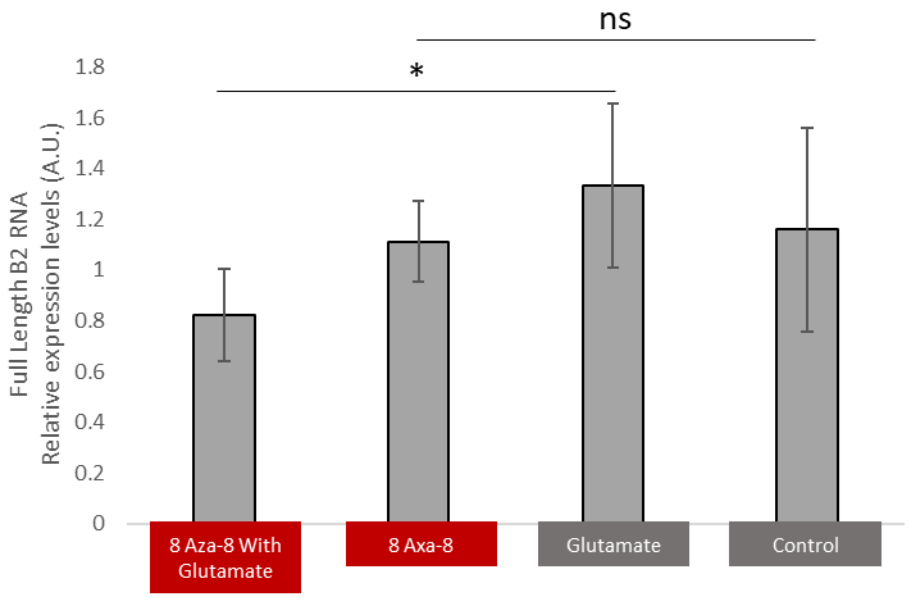

Figure 3.20: Full-length B2 RNA expression following incubation with 8-Azaadenosine and glutamate cellular stress. HT22 cell line. Gene expression was determined using a relative standard curve of HPRT. The HT22 cells were incubated with 8-AzaAdenosine for 24 hours followed by 6 hours with a 1µM final concentration of glutamate. All steps were performed with cells at 37 ^{o}C. Represents the Mean value of the group (* = p=0.02 1-tailed paired t-test) (ns = not significant) n=4 (n represents number of independent experiments).

3.3.3 Inhibition of editing by 8-AzaA shows an additive affect in P53 RNA transcripts

We then examined a factor connected with cell death to confirm that indeed in our system we had achieved a sufficient level of cellular stress. P53 was checked within the same cells for its overall expression levels, which are also linked to the cellular stress response. Figure 3.21 shows that 8-AzaA (reduced A to I editing) shows a significant effect on the expression level of P53 transcript when exposed to glutamate toxicity. Furthermore, we confirmed that 1 µM glutamate stress is of significant stress in control cells to cause an increase in the pro-apoptotic factor P53. In conclusion, although further work may be needed to determine the overall impact that Adenosine to Inosine editing plays on the stress response, inhibition of the ADAR1 enzyme activity and its linked reduction in A to I editing directly result in the processing of SINE RNA

during cellular stress and increase of cell death markers like P53. In contrast, during cellular stress a reduction in A to I transitions results in an overall reduction of cell death markers.

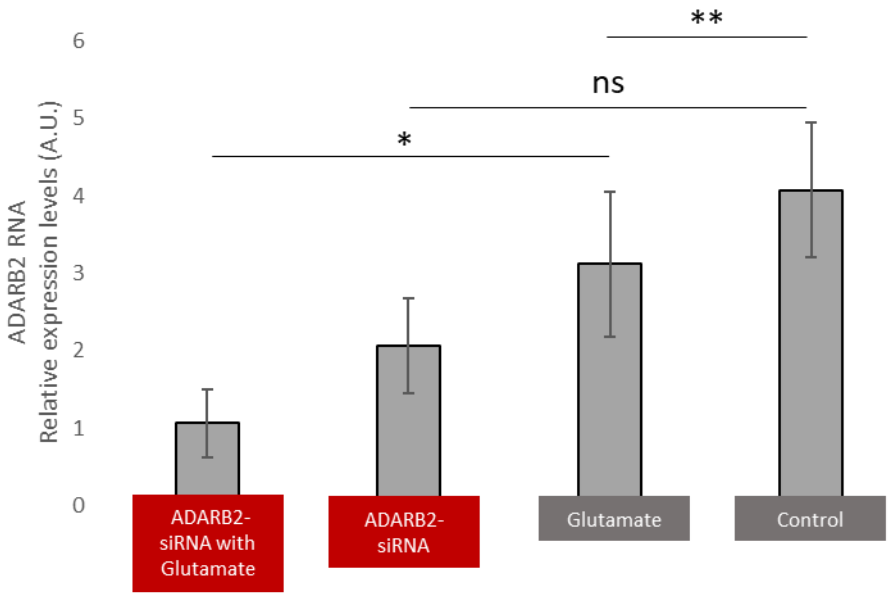

Figure 3.21: P53 RNA expression following incubation with 8-Azaadenosine and glutamate cellular stress. HT22 cell line. Gene expression was determined using a relative standard curve of HPRT. The HT22 cells were incubated with 8-AzaAdenosine for 24 hours followed by 6 hours with a 1 µM final concentration of glutamate. All steps were performed with cells at 37 ^{o}C. Represents the Mean value of the group (* = p = 0.01 1-tailed paired t-test) (** = p = 0.006 1 tailed paired t-test) (ns = not significant) n=4 (n represents number of independent experiment).

Chapter 4

Discussion

4.1 Overview

In vitro experiments investigating the impact of A to I editing on RNA stability depend on the generation of edited RNAs at specific positions. Employment of ADAR enzymes and incubation with IVT RNAs could deliver such products but these would be nonspecific involving modifications simultaneously at multiple positions. Investigation of the impact of editing at specific positions (such as position 49 in our case) requires an alternative approach that allows targeted RNA synthesis such as solid-phase synthesis. However, this approach is not optimized for long RNAs such as B2 RNA. Thus, optimization of RNA solid-phase synthesis and specifically synthesis involving the addition of Inosine is critical to understanding the role that Adenosine to Inosine editing interplays with B2 RNA. To this end, in the current Thesis, several challenges had to be overcome through a multitude of optimizations that had to be made throughout this process to allow for the generation of such edited B2 RNA. These improvements include length optimizations, protocol time adjustments (for example in coupling), and extensive priming of the synthesizer. Overall, we were able to extend the capability of the RNA synthesis to modified RNAs greater than 40 bases and we were able to directly infer the effects of Inosine modification on the B2 SINE RNA. Our results confirmed our hypothesis that A to I editing leads to the stabilization of B2 RNAs.

Furthermore, cell culture assays on the effects that A to I editing has on the stability and therefore processing of the B2 SINE RNA confirmed also in a cell culture model the protective

effect of Inosines on SINE B2 RNA by our prior in vivo data and the in vitro data of the current thesis. Initially, the knockdown of ADARB2 proved to be cofounded by the application of cellular stress. Thus, the decision to change direction and instead decrease overall A to I editing was made. The reduction of A to I editing through the use of the small molecule inhibitor 8-AzaA demonstrates a protective effect of Inosine modification on full-length B2. This effect can be seen only during cellular stress as during glutamate toxicity stress the loss of A to I editing results in a greater increase from the control in the overall processing of B2 than in non-stress conditions.

4.2 Optimizations leading to improved performance of modified long-range RNA solid-phase synthesis.

Solid-phase RNA synthesis enables the synthesis of RNAs for further downstream studies to understand the role of RNA modifications and their direct impact on the function and structure of RNA molecules. These insights into the world of RNA allow for a deeper look into the epitranscriptomic changes that play a major role in the cell. However, to allow for accurate and efficient usage of RNA synthesis technology optimization of synthesis is an important factor, as both a cost-reducing and an improvement in overall accuracy and yield.

Optimal RNA synthesis is usually possible only for fewer than forty base pairs despite longer sequences being important to further our understanding of complex RNA molecules when talking about modifications. In this thesis, initially, long RNA synthesis resulted in a major loss of yield as the segment progressed over the long synthesis time (Figure 3.1). This drop-in efficacy is likely a result of compounding step-by-step yield where bases fail to bind and there is an overall reduction in total yield as a result. To address this, we increased the coupling time for each base

from 360 seconds to 800 seconds, providing more time for each base to bind to see improvement in the step-by-step yield combined with further optimizing the length of synthesized sequences from the 100bp test sequences to 60bp B2 fragments. Secondly, the use of RNA amides at room temperature during the greater than 24 hours synthesis period results in the efficiency being reduced due to the RNA amides losing their binding efficiency while sitting at room temperature.

The efficacy of the RNA amides was improved by the modification of the device setting and reduction of the temperature over the entire synthesis time. These improvements resulted in overall increased efficiency as shown in Figure 3.8, however, with the addition of inosine modifications to the synthesis protocol, new optimizations were required, as inosine amides have lower binding capacity. Initially, reducing the number of inosine bases per sequence was suggested as a potential way to increase overall yield however as shown in Figure 3.10 synthesis still does come with a significant loss in yield. Thus, the increased priming of the device with the addition of a sacrificial sequence to prime the synthesizer was developed to ensure proper quantities of amides reach the column. This final optimization resulted in a great increase in the overall efficiency of synthesis as shown in Figure 3.11.

4.2 Role of Adenosine to Inosine editing and B2 in stress response

The cellular stress response is very important and ultimately fundamental to life. Thus, understanding how the stress response works are critical to our understanding of molecular mechanisms underlying health and disease. To this end, a complete understanding of the ADAR family of enzymes and the adenosine to inosine modifications they induce would provide insights into cellular stress. As demonstrated by Zovoilis et al. (Zovoilis et al. 2016), B2 SINE RNA plays a

major role in the cellular response to heat shock, thus, the stability of RNA such as B2 may provide an important factor in the cells' ability to respond to stress. In addition, A to I editing by the ADAR enzymes is disproportionally found in intronic regions of RNA specifically in that of the SINE elements, leading to a need to understand the roles they may play in stabilizing SINE RNA and the important roles they have in cellular stresses.

4.3 ADARB2 siRNA Knockdown Assay

During cellular stress such as with glutamate in Figure 3.17 we see a significant reduction in ADARB2 levels. Thus, the use of anti-ADARB2 in Figure 3.17 revealed the effectiveness of siRNA as a tool for the knockdown of ADARB2 but also the limitations of its usefulness in our context, due to its association with cell stress preventing its use in a cellular stress model.

4.4 Decoding the effects of 8-azaAdenosine on B2 RNA levels

An overall reduction in full-length B2 RNA during cellular stress and the inhibition of ADAR by 8-AzaA suggests a link between cellular stress response of B2 processing and the A to I editing as shown in Figure 3.18. The reduction in A to I editing may induce a change in the overall stability of B2 creating an increase in overall processing while potentially also impacting the overall transportation of mRNA transcripts. Furthermore, as shown previously (Zovoilis et al. 2016) the ability of processed B2 RNA to alter the transcription of stress response genes is essential to the cellular stress response, thus, changes in full-length B2 RNA may have a dramatic impact on the ability of cells to deal with cellular stress.

4.5 Hsf-1 Processing of full-length B2 RNA

The presence of Inosine in B2 samples seems to suggest increased stability for the RNA transcript. As seen in Figure 3.14 when incubated with HSF-1 the addition of Inosine seems to suggest a protective effect resulting in a reduced speed at which HSF-1 can process the full-length B2 RNA resulting in 20.7% of the inosine modified B2 remaining in contract to the 14.9% of the control B2 RNA lacking the presence of the A to I conversion at position 49. These results agree with our labs' *in vivo* results that imply a protective role of editing on B2 RNA levels during amyloid beta toxicity.

4.6 Future Directions

Overall, we have shown a link between the addition of Inosine into RNA and the stability of that RNA. Specifically, the addition of an Inosine into the 49^{th} position of B2 SINE RNA may be key in understanding the differing editing profiles of this RNA during cellular stress. This overall change instability from a single position requires further research to determine if the change of stability is a conformational change as a result of the addition of the Inosine.

Initially, additional B2 SINE RNA would need to be made with inosine additions at a variety of other locations that show high levels of editing along with further work into making sequences with multiple edits. This would allow for a greater understanding of the effects that the addition of inosine makes on SINE RNA stability. Furthermore, the creation of ALU SINE RNA with similar edits would be essential to confirm this stability effect on human SINE RNA in addition to the mouse B2 SINES.

Furthermore, more work needs to be done regarding optimizing the K&A synthesizer to allow for the creation of many more A to I edited sequences to allow the continuation of this work. For example, further optimization of the timings along with the addition of sacrificial sequences that run throughout the synthesis would allow the lesser-used bases to be primed to allow for maximum efficiency of synthesis.

Overall, the above-mentioned future work will allow for a greater understanding of the effects that A to I editing and to the effect the ADAR family of enzymes have on the stability and processing of SINE RNA. This may lead to implications on ways to protect SINE RNA from self-cleavage and degradation from enzymes such as HSF-1 which may lead to potential therapeutic opportunities for disorders that may be linked such as Alzheimer's Disease.

Chapter 5

Conclusions

In conclusion, this work demonstrates a connection between adenosine to inosine editing catalyzed by the ADAR family of enzymes and the overall stability of SINE RNA specifically that of the mouse B2 SINE RNA. Along with demonstrating a novel use for RNA synthesis to create *in vitro* editing of RNA sequences to mimic the same editing profiles found within *in vivo* samples.

We know that B2 SINE RNAs are processed during cellular response to stress by enzymes such as Hsf-1 (Zovoilis et al. 2016). Thus, the finding that the SINE B2 processing effects can be reduced by the addition of inosines reveals the importance of A to I editing in SINE RNA regulation of gene expression. This effect of editing on B2 RNA processing provides an improved understanding of the potential role of RNA modification in disease by regulating the overall loss of full-length B2 transcripts and the transcriptional regulation they are responsible for. Thus, having the potential to impact gene expression across many different cellular stress contexts and diseases could have potential therapeutic implications. Future research into the role of adenosine to inosine editing in SINE RNA may reveal new therapeutic targets and give a greater understanding of the role that SINE RNA plays in Alzheimer's Disease.

References

Advanced Chemistry Development I. 2021. ACD/ChemSketch, version 2020.2.1. Toronto, On, Canada, www.acdlabs.com.

Agrawal N, Dasaradhi PV, Mohmmed A, Malhotra P, Bhatnagar RK, Mukherjee SK. 2003. RNA interference: biology, mechanism, and applications. Microbiol Mol Biol Rev 67:657-685.

Andersen JV, Schousboe A, Verkhratsky A. 2022. Astrocyte energy and neurotransmitter metabolism in Alzheimer's disease: integration of the glutamate/GABA-glutamine cycle. Prog Neurobiol:102331.

Barbieri I, Kouzarides T. 2020. Role of RNA modifications in cancer. Nat Rev Cancer 20:303-322.

Batzer MA, Deininger PL. 2002. Alu repeats and human genomic diversity. Nat Rev Genet 3:370-379.

Beck CR, Garcia-Perez JL, Badge RM, Moran JV. 2011. LINE-1 elements in structural variation and disease. Annu Rev Genomics Hum Genet 12:187-215.

Boccaletto P, et al. 2018. MODOMICS: a database of RNA modification pathways. 2017 update. Nucleic Acids Res 46:D303-D307.

Bodea GO, McKelvey EGZ, Faulkner GJ. 2018. Retrotransposon-induced mosaicism in the neural genome. Open Biol 8.

Borodulina OR, Kramerov DA. 2008. Transcripts synthesized by RNA polymerase III can be polyadenylated in an AAUAAA-dependent manner. RNA 14:1865-1873.

Brachova P, Alvarez NS, Hong X, Gunewardena S, Vincent KA, Latham KE, Christenson LK. 2019. Inosine RNA modifications are enriched at the codon wobble position in mouse oocytes and eggsdagger. Biol Reprod 101:938-949.

Carroll ML, et al. 2001. Large-scale analysis of the Alu Ya5 and Yb8 subfamilies and their contribution to human genomic diversity. J Mol Biol 311:17-40.

Cech TR, Steitz JA. 2014. The noncoding RNA revolution-trashing old rules to forge new ones. Cell 157:77-94.

Charette M, Gray MW. 2000. Pseudouridine in RNA: what, where, how, and why. IUBMB Life 49:341-351.

Chen LL, Carmichael GG. 2008. Gene regulation by SINES and inosines: biological consequences of A-to-I editing of Alu element inverted repeats. Cell Cycle 7:3294-3301.

Cheng Y, Saville L, Gollen B, Isaac C, Belay A, Mehla J, Patel K, Thakor N, Mohajerani MH, Zovoilis A. 2020. Increased processing of SINE B2 ncRNAs unveils a novel type of transcriptome deregulation in amyloid beta neuropathology. Elife 9.

Cheng Y, Saville L, Gollen B, Veronesi AA, Mohajerani M, Joseph JT, Zovoilis A. 2021. Increased Alu RNA processing in Alzheimer brains is linked to gene expression changes. EMBO Rep 22:e52255.

Correia de Sousa M, Gjorgjieva M, Dolicka D, Sobolewski C, Foti M. 2019. Deciphering miRNAs' Action through miRNA Editing. Int J Mol Sci 20.

Daniels GR, Deininger PL. 1985. Repeat sequence families derived from mammalian tRNA genes. Nature 317:819-822.

Dominissini D, et al. 2016. The dynamic N(1)-methyladenosine methylome in eukaryotic messenger RNA. Nature 530:441-446.

Eggington JM, Greene T, Bass BL. 2011. Predicting sites of ADAR editing in double-stranded RNA. Nat Commun 2:319.

Elbarbary RA, Lucas BA, Maquat LE. 2016. Retrotransposons as regulators of gene expression. Science 351:aac7247.

Fasolo F, et al. 2019. The RNA-binding protein ILF3 binds to transposable element sequences in SINEUP lncRNAs. FASEB J 33:13572-13589.

Gadhave K, Kapuganti SK, Mishra PM, Giri R. 2022. p53 TAD2 Domain (38-61) Forms Amyloid-like Aggregates in Isolation. ACS Chem Neurosci.

Gavrilov K, Saltzman WM. 2012. Therapeutic siRNA: principles, challenges, and strategies. Yale J Biol Med 85:187-200.
Helm M, Motorin Y. 2017. Detecting RNA modifications in the epitranscriptome: predict and validate. Nat Rev Genet 18:275-291.
Hernandez AJ, Zovoilis A, Cifuentes-Rojas C, Han L, Bujisic B, Lee JT. 2020. B2 and ALU retrotransposons are self-cleaving ribozymes whose activity is enhanced by EZH2. Proc Natl Acad Sci U S A 117:415-425.
Hong H, Lin JS, Chen L. 2015. Regulatory factors governing adenosine-to-inosine (A-to-I) RNA editing. Biosci Rep 35.
Jia G, Fu Y, He C. 2013. Reversible RNA adenosine methylation in biological regulation. Trends Genet 29:108-115.
Jonkhout N, Tran J, Smith MA, Schonrock N, Mattick JS, Novoa EM. 2017. The RNA modification landscape in human disease. RNA 23:1754-1769.
Karijolich J, Zhao Y, Alla R, Glaunsinger B. 2017. Genome-wide mapping of infection-induced SINE RNAs reveals a role in selective mRNA export. Nucleic Acids Res 45:6194-6208.
Li Y, Gohl M, Ke K, Vanderwal CD, Spitale RC. 2019. Identification of Adenosine-to-Inosine RNA Editing with Acrylonitrile Reagents. Org Lett 21:7948-7951.
Licht K, Hartl M, Amman F, Anrather D, Janisiw MP, Jantsch MF. 2019. Inosine induces context-dependent recoding and translational stalling. Nucleic Acids Res 47:3-14.
Liu G, et al. 2019. Adenosine deaminase acting on RNA-1 (ADAR1) inhibits hepatitis B virus (HBV) replication by enhancing microRNA-122 processing. J Biol Chem 294:14043-14054.
Mallela A, Nishikura K. 2012. A-to-I editing of protein coding and noncoding RNAs. Crit Rev Biochem Mol Biol 47:493-501.
Mattick JS, Makunin IV. 2006. Non-coding RNA. Hum Mol Genet 15 Spec No 1:R17-29.
Mladenova D, et al. 2018. Adar3 Is Involved in Learning and Memory in Mice. Front Neurosci 12:243.
Moore S, et al. 2019. ADAR2 mislocalization and widespread RNA editing aberrations in C9orf72-mediated ALS/FTD. Acta Neuropathol 138:49-65.
Netzband R, Pager CT. 2020. Epitranscriptomic marks: Emerging modulators of RNA virus gene expression. Wiley Interdiscip Rev RNA 11:e1576.
Nishikura K. 2010. Functions and regulation of RNA editing by ADAR deaminases. Annu Rev Biochem 79:321-349.
- 2016. A-to-I editing of coding and non-coding RNAs by ADARs. Nat Rev Mol Cell Biol 17:83-96.
Ota H, Sakurai M, Gupta R, Valente L, Wulff BE, Ariyoshi K, Iizasa H, Davuluri RV, Nishikura K. 2013. ADAR1 forms a complex with Dicer to promote microRNA processing and RNA-induced gene silencing. Cell 153:575-589.
Perks KL, et al. 2018. PTCD1 Is Required for 16S rRNA Maturation Complex Stability and Mitochondrial Ribosome Assembly. Cell Rep 23:127-142.
Pertea M. 2012. The human transcriptome: an unfinished story. Genes (Basel) 3:344-360.
Phizicky EM, Hopper AK. 2010. tRNA biology charges to the front. Genes Dev 24:1832-1860.
Reynolds A, Leake D, Boese Q, Scaringe S, Marshall WS, Khvorova A. 2004. Rational siRNA design for RNA interference. Nat Biotechnol 22:326-330.
Richardson SR, Doucet AJ, Kopera HC, Moldovan JB, Garcia-Perez JL, Moran JV. 2015. The Influence of LINE-1 and SINE Retrotransposons on Mammalian Genomes. Microbiol Spectr 3:MDNA3-0061-2014.
Roundtree IA, Evans ME, Pan T, He C. 2017. Dynamic RNA Modifications in Gene Expression Regulation. Cell 169:1187-1200.
Salem AH, Kilroy GE, Watkins WS, Jorde LB, Batzer MA. 2003. Recently integrated Alu elements and human genomic diversity. Mol Biol Evol 20:1349-1361.
Samuel CE. 2001. Antiviral actions of interferons. Clin Microbiol Rev 14:778-809, table of contents.

Santer L, et al. 2019. Circulating Long Noncoding RNA LIPCAR Predicts Heart Failure Outcomes in Patients Without Chronic Kidney Disease. Hypertension 73:820-828.
Soll D. 1971. Enzymatic modification of transfer RNA. Science 173:293-299.
Squires JE, Patel HR, Nousch M, Sibbritt T, Humphreys DT, Parker BJ, Suter CM, Preiss T. 2012. Widespread occurrence of 5-methylcytosine in human coding and non-coding RNA. Nucleic Acids Res 40:5023-5033.
Sun T, Wu R, Ming L. 2019. The role of m6A RNA methylation in cancer. Biomed Pharmacother 112:108613.
Sun T, et al. 2021. Decoupling expression and editing preferences of ADAR1 p150 and p110 isoforms. Proc Natl Acad Sci U S A 118.
Teichert I. 2018. Adenosine to inosine mRNA editing in fungi and how it may relate to fungal pathogenesis. PLoS Pathog 14:e1007231.
Tucker JM, Glaunsinger BA. 2017. Host Noncoding Retrotransposons Induced by DNA Viruses: a SINE of Infection? J Virol 91.
Uhlen M, et al. 2015. Proteomics. Tissue-based map of the human proteome. Science 347:1260419.
Ustyantsev IG, Borodulina OR, Kramerov DA. 2020a. Identification of nucleotide sequences and some proteins involved in polyadenylation of RNA transcribed by Pol III from SINEs. RNA Biol:1-14.
Ustyantsev IG, Tatosyan KA, Stasenko DV, Kochanova NY, Borodulina OR, Kramerov DA. 2020b. [Polyadenylation of Sine Transcripts Generated by RNA Polymerase III Dramatically Prolongs Their Lifetime in Cells]. Mol Biol (Mosk) 54:78-86.
Walkley CR, Li JB. 2017. Rewriting the transcriptome: adenosine-to-inosine RNA editing by ADARs. Genome Biol 18:205.
Weiner AM. 2002. SINEs and LINEs: the art of biting the hand that feeds you. Curr Opin Cell Biol 14:343-350.
Wilusz JE, Sunwoo H, Spector DL. 2009. Long noncoding RNAs: functional surprises from the RNA world. Genes Dev 23:1494-1504.
Wright DJ, Force CR, Znosko BM. 2018. Stability of RNA duplexes containing inosine.cytosine pairs. Nucleic Acids Res 46:12099-12108.
Xing YH, Chen LL. 2018. Processing and roles of snoRNA-ended long noncoding RNAs. Crit Rev Biochem Mol Biol 53:596-606.
Xu LD, Ohman M. 2018. ADAR1 Editing and its Role in Cancer. Genes (Basel) 10.
Yan Q, Zhu C, Guang S, Feng X. 2019. The Functions of Non-coding RNAs in rRNA Regulation. Front Genet 10:290.
Yang L, Scott L, Wichman HA. 2019. Tracing the history of LINE and SINE extinction in sigmodontine rodents. Mob DNA 10:22.
Yang Y, Zhou X, Jin Y. 2013. ADAR-mediated RNA editing in non-coding RNA sequences. Sci China Life Sci 56:944-952.
Yu L, Zhang YP. 2005. Evolutionary implications of multiple SINE insertions in an intronic region from diverse mammals. Mamm Genome 16:651-660.
Zhang L, Lu Q, Chang C. 2020. Epigenetics in Health and Disease. Adv Exp Med Biol 1253:3-55.
Zhao BS, Roundtree IA, He C. 2017. Post-transcriptional gene regulation by mRNA modifications. Nat Rev Mol Cell Biol 18:31-42.
Zhao LY, Song J, Liu Y, Song CX, Yi C. 2020. Mapping the epigenetic modifications of DNA and RNA. Protein Cell 11:792-808.
Zhou R, Yao W, Xie C, Zhang L, Pei Y, Li H, Feng Z, Yang Y, Li K. 2020. Developmental stage-specific A-to-I editing pattern in the postnatal pineal gland of pigs (Sus scrofa). J Anim Sci Biotechnol 11:90.
Zovoilis A, Cifuentes-Rojas C, Chu HP, Hernandez AJ, Lee JT. 2016. Destabilization of B2 RNA by EZH2 Activates the Stress Response. Cell 167:1788-1802 e1713.

Appendix

Table A.1: RNA Sequences used for RNA synthesis

Sequence ID	**Sequence 5’-3’**
100BPOZ	GCCGGGCGTGGTGGCGGGCGCCTGTAGTCCCAGCTACTCGG GAGGCTGAGGCAGGAGAATGGCGTGAACCCGGGAGGCGGAG CTTGCAGTGAGCCGAGAT
B21-60	GGGGGCTGAGATGGCTCAGTGGGTAAGAGCACCCGACTGCTCTTCCGAAGGTCCGG AGTTC
B21-60I	GGGGGCTGAGATGGCTCAGTGGGTA**I**GAGC**I**CCCGACTGCTCTTCCGA**I**GGTCCGGA GTTC
B21-60O	GGGGGCTGAGATGGCTCAGTGGGTAAGAGCACCCGACTGCTCTTCCGA**I**GGTCCGG AGTTC
B2CT3END	GGGGCTGGTGAGATGGCTCAGTGGGTAAGAGCACCCGACTGCTCTTCCG AAGGTCCGGAGTTCAAATCCCAGCAACCACA
B2CT5END	TGGTGGCTCACAACCATCCGTAACGAGATCTGACTCCCTCTTCTGG AGTGTCTGAAGACAGCTACAGTGTACTTACATATAATAAATAAATAAATCTT TA
B2RNAI	GGGGCTGGTGAGATGGCTCAGTGGGTAAGAGCACCCGACTGCTCTT CCGAAGGTCCGGAGTTCAAATCCCAGCAACCACATGGTGGCTCACAA CCATCCGTAACGAGATCTGACTCCCTCTTCTGGAGTGTCTGAAGACA GCTACAGTGTACTTACATATAATAAATAAATAAATCTTTA
B2RNA	GGGGGCTGAGATGGCTCAGTGGGTAAGAGCACCCGACTGCTCTTCCGA AGGTCCGGAGTTCAAATCCCAGCAACCACATGGTGGCTCACA**I**CCATC CGTAACGAGATCTG**I**CTCCCTCTTCTGGAGTGTCTGA**I**GACAGCTACA GTGTACTTACATATAATAAATAAATAAATCTTTA

Table A.2: Nucleic acid reagents used for the in vitro transcription of 61-182 B2 RNA

Sequence ID	**Sequence 5’-3’**
T7 Forward	TAATACGACTCACTATAG
B2 Reverse Primer	TTTTTTTTAAAGATTTATTTATTTATTATATGTAAGTACA
B2 61-182 Containing T7 promoter	ATTAGCTGAGTGATATCTCAAATCCCAGCAACCACATGGTGGCTCACAACC ATCCGTAACGAGATCTGACTCCCTCTTCTGGAGTGTCTGAAGACAGCTACAG TGTACTTACATATAATAAATAAATAAATCTTTAAAA

Table A.3: Mouse Nucleic acid Primers used for qPCR

Sequence ID	Sequence 5'-3'
HPRT - Forward	TCCTCCTCAGACCGCTTTT
HPRT - Reverse	CCTGGTTCATCATCGCTAATC
B2 - Forward	GGGGCTGGTGAGATG
B2 - Reverse	AGCTGTCTTCAGACACTC C
P53 - Forward	AAACGCTTCGAGATGTTCCG
P53 - Reverse	GTAGACTGGCCCTTCTTGGT

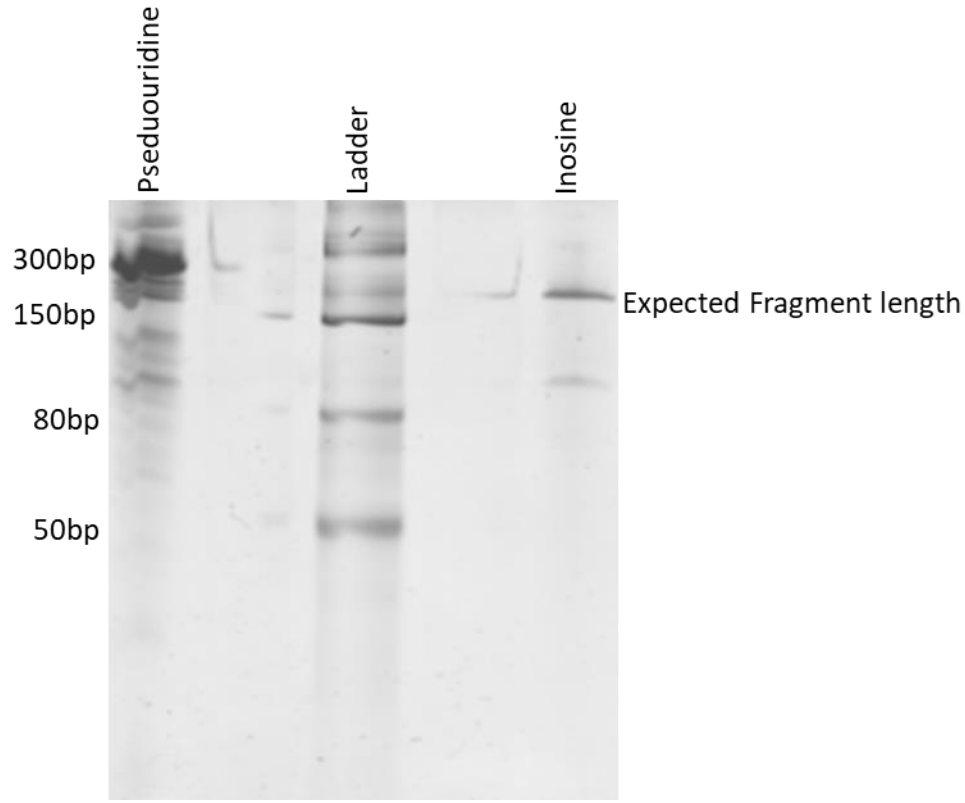

Figure A.1: Urea-PAGE of gel containing IVT samples with modified bases by replacement of corresponding bases in IVT's Base master mix with the modified version (U- Pseuduouridine, A-Inosine (ITP)). IVT results in full-length B2 with a base completely replaced with a modified version as per the B2 IVT reference sequence containing the T7 promoter.

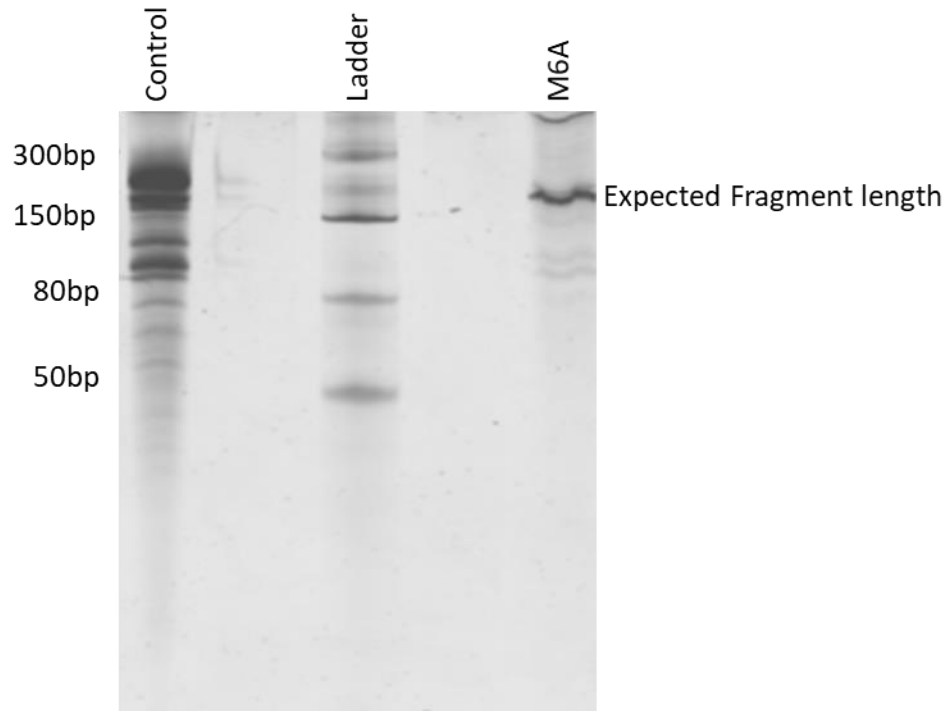

Figure A.2: Urea-PAGE of gel containing IVT samples with modified bases by replacement of corresponding bases in IVT's Base master mix with the modified version (A- M6A). IVT results in full-length B2 with a base completely replaced with a modified version as per the B2 IVT reference sequence containing the T7 promoter.

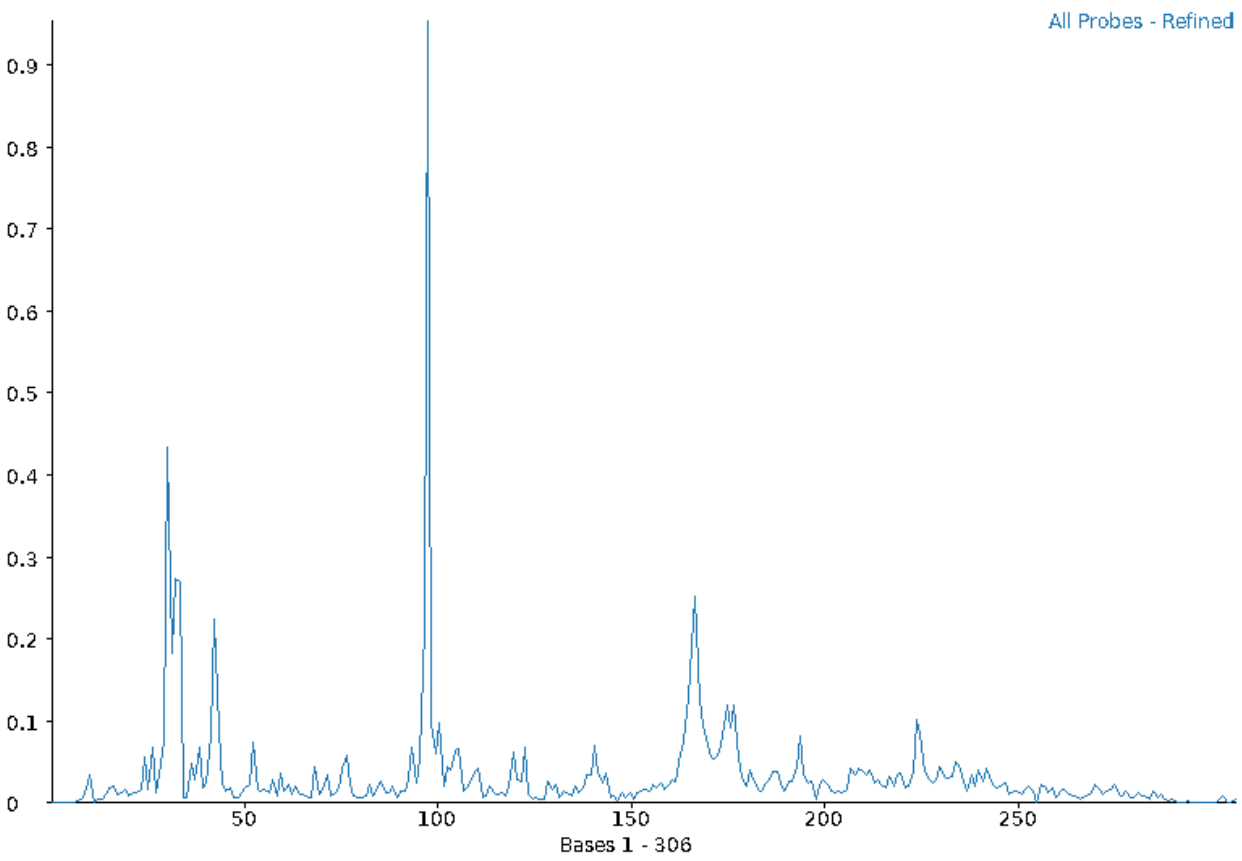

Figure A.3 Locations of previously identified Inosine locations within mapped against the location of AluY throughout the genome using seqmonk. Bases represent AluY (-5) - 300 bp from the transcriptional start site. Mapped to Hg-38

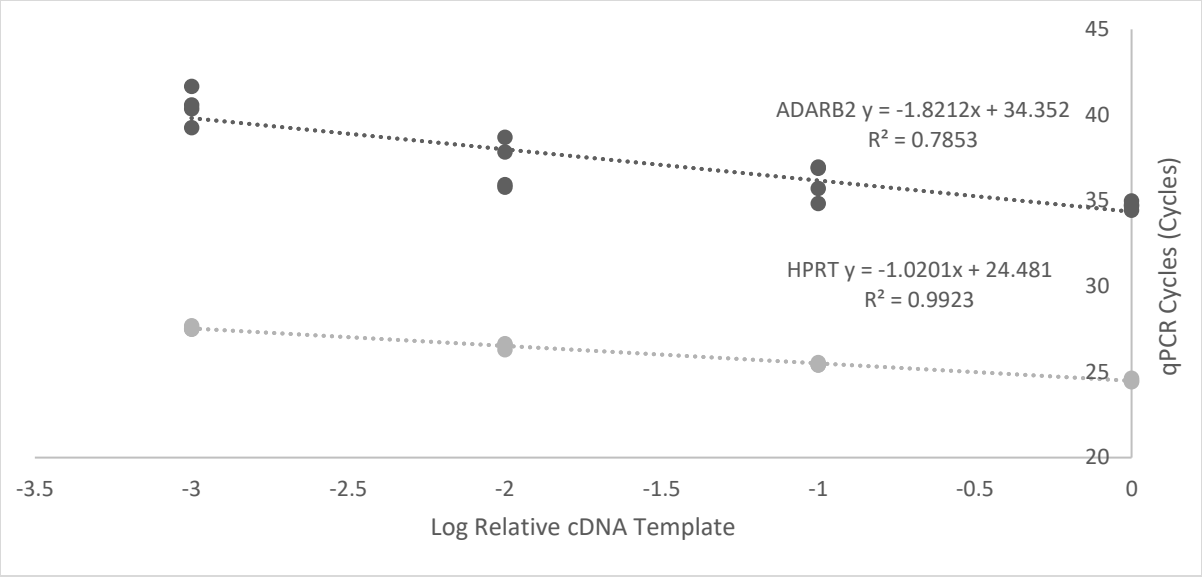

Figure A.4 Standard Curve from qPCR of HT-22 mouse cell line showing very low quantities of ADARB2 transcripts. Resulting in high variability among individual samples.